

1 **Regional heterogeneities in the emission of airborne primary sugar**
2 **compounds and biogenic secondary organic aerosols in the East Asian**
3 **outflow: Evidence for coal combustion as a source of levoglucosan**

4

5 **M. Mozammel Haque^{1,2,3}, Yanlin Zhang^{1,2*} Srinivas Bikkina⁴, Meehye Lee⁵, and Kimitaka**
6 **Kawamura^{3,4*}**

7

8 *¹Yale-NUIST Center on Atmospheric Environment, International Joint Laboratory on Climate and*
9 *Environment Change (ILCEC), Nanjing University of Information Science & Technology, Nanjing,*
10 *210044, China*

11 *²School of Applied Meteorology, Nanjing University of Information Science & Technology, Nanjing*
12 *210044, China*

13 *³Institute of Low Temperature Science, Hokkaido University, Sapporo 060-0819, Japan*

14 *⁴Chubu Institute for Advanced Studies, Chubu University, Kasugai 487-8501, Japan*

15 *⁵Department of Earth and Environmental Sciences, Korea University, Anam-dong, Sungbuk-gu, Seoul*
16 *136-701, South Korea*

17

18

19

20

21

22

23

24

25

26

27 **Corresponding author*

28 E-mail: dryanlinzhang@outlook.com (Yan-Lin Zhang)

29 E-mail: kkawamura@isc.chubu.ac.jp (Kimitaka Kawamura)

30

31 **ABSTRACT**

32 Biomass burning (BB) significantly influences the chemical composition of organic aerosols
33 (OA) in the East Asian outflow. Source apportionment of BB-derived OA is an influential
34 factor for understanding their regional emissions, which is crucial for reducing uncertainties
35 in their projected climate and health-effects. We analyzed here three different classes of
36 atmospheric sugar compounds (anhydrosugars, primary sugars, and sugar alcohols) and two
37 types of biogenic secondary organic aerosol (BSOA) tracers (isoprene- and monoterpene
38 derived SOA products) in a year-long collected total suspended particulate matter (TSP) from
39 an island-based receptor site in South Korea, Gosan. We investigate seasonal variations in the
40 source emissions of BB-derived OA using mass concentrations of anhydrosugars and
41 radiocarbon (^{14}C -) isotopic composition of organic carbon (OC) and elemental carbon (EC) in
42 ambient aerosols. Levoglucosan (*Lev*) is the most abundant anhydrosugar, followed by
43 galactosan (*Gal*) and mannosan (*Man*). Strong correlations of *Lev* with *Gal* and *Man*, along
44 with their ratios (*Lev/Gal*: 6.65 ± 2.26 ; *Lev/Man*: 15.1 ± 6.76) indicate the contribution from
45 hardwood burning emissions. The seasonal trends revealed that the BB impact is more
46 pronounced in winter and fall, as evidenced by the high concentrations of anhydrosugars.
47 Likewise, significant correlations among three primary sugars (i.e., glucose, fructose, and
48 sucrose) emphasized the contribution of airborne pollen. The primary sugars showed higher
49 concentrations in spring/summer than winter/fall. The fungal spore tracer compounds (i.e.,
50 arabitol, mannitol, and erythritol) correlated well with trehalose (i.e., a proxy for soil organic
51 carbon), suggesting the origin from airborne fungal spores and soil microbes in the East
52 Asian outflow. These sugar alcohols peaked in summer, followed by spring/fall and winter.
53 Monoterpene-derived SOA tracers were most abundant compared to isoprene-SOA tracers.
54 Both BSOA tracers were dominant in summer, followed by fall, spring, and winter. The
55 source apportionment based on multiple linear regressions and diagnostic mass ratios
56 together revealed that BB emission mostly contributed from hardwood and crop-residue
57 burning. We also found significant positive linear relationships of ^{14}C -based nonfossil- and
58 fossil-derived organic carbon fractions with *Lev-C* along with the comparable regression
59 slopes, suggesting the importance of BB and coal combustion sources in the East Asian
60 outflow.

61

62 **Keywords:** Biomass burning tracers, primary biological aerosol particles, biogenic SOA
63 tracers, radiocarbon-based source apportionment, organic aerosols, East Asian outflow

64 1. Introduction

65 Organic aerosols (OA), which account for a major fraction of up to 50% of airborne total
66 suspended particulate matter, have considerable effects on regional and global climate by
67 absorbing or scattering sunlight (Kanakidou et al., 2005). However, the climate effects of OA
68 are involved with large uncertainties due to our limited understanding of the contributing
69 sources. OA can be derived from both primary emissions and secondarily formed species.
70 Sugars are an important group of water-soluble, primary organic compounds whose
71 concentrations are significant in atmospheric aerosols over the continent (Jia and Fraser,
72 2011; Fu et al., 2008; Yttri et al., 2007; Graham et al., 2003). Anhydrosugars such as
73 levoglucosan, galactosan, and mannosan are the key tracers of biomass burning (BB)
74 emissions (Simoneit, 2002). Sugar alcohols, along with glucose, trehalose and sucrose are
75 mostly originated from primary biological particles such as fungal spores, pollen, bacteria,
76 viruses, and vegetative debris (Graham et al., 2003; Simoneit et al., 2004a; Bauer et al., 2008;
77 Deguillaume et al., 2008). Primary sugars and sugar alcohols are predominantly present in the
78 coarse mode aerosols, accounting for 0.5-10% of atmospheric aerosol carbon matter (Yttri et
79 al., 2007; Pio et al., 2008).

80 Secondary organic aerosol (SOA) is a large fraction of OA, while there were only
81 limited studies about the key factors controlling SOA formation. The SOA formation
82 significantly increases with the enhancement of the ambient aerosol mass (Liu et al., 2018).
83 SOA is formed by both homogenous and heterogeneous reactions of volatile organic
84 compounds (VOCs) in the atmosphere (Surratt et al., 2010; Robinson et al., 2007; Claeys et
85 al., 2004). On a global estimation, biogenic VOCs (BVOCs) such as isoprene, monoterpenes
86 (e.g., α/β -pinene), and sesquiterpenes (e.g., β -caryophyllene) are one order of magnitude
87 higher than those of anthropogenic VOCs (e.g., toluene) (Guenther et al., 2006). The global
88 emissions of annual BVOCs were estimated to be 1150 TgC yr⁻¹, accounting for 44%
89 isoprene and 11% monoterpenes (Guenther et al., 1995). Isoprene is highly reactive and
90 promptly reacts with oxidants such as O₃, OH, and NO_x in the atmosphere to form SOA
91 (Kroll et al., 2005, 2006; Ng et al., 2008; Surratt et al., 2010; Bikkina et al., 2021), estimated
92 to be 19.2 TgC yr⁻¹, consisting of ~70% of the total SOA budget (Heald et al., 2008).
93 Monoterpenes are important sources of biogenic secondary organic aerosol (BSOA),
94 considering α -pinene as major species, accounting for ~35% of the global monoterpenes
95 emissions (Griffin et al., 1999).

96 Anthropogenic activities such as coal and biofuel combustion over East Asia,
97 including China, are responsible for the vast emission of OA (Huebert et al., 2003; Zhang et

98 al., 2016). Understanding the ambient levels OA in the East Asian outflow is crucial for
99 assessing their regional climatic effects. As part of this effort, the Korean Climate
100 Observatory at Gosan (KCOG), a supersite located in South Korea, is an ideal location for
101 investigating the atmospheric outflow characteristics from East Asia (Fu et al., 2010a; Kundu
102 et al., 2010; Ramanathan et al., 2007; Kawamura et al., 2004; Arimoto et al., 1996). For
103 instance, primary OA associated with soil/desert dust in East Asia, along with forest fires in
104 Siberia/northeastern China, are transported over Gosan in spring (Wang et al., 2009a). BSOA
105 during long-range transport from the continent and open ocean, as well as local vegetation,
106 can significantly contribute to Gosan aerosols. Although these investigations were carried out
107 almost a decade ago, no such observations are available in contemporary times from Gosan.
108 Here, we attempt to understand the current states of East Asian OA using both the molecular
109 marker approach and radiocarbon data of carbonaceous components.

110 The KCOG, located on the western side of Jeju Island adjacent to the Yellow Sea and
111 the East China Sea, is facing the Asian continent but is isolated from public areas of the
112 island (Kawamura et al., 2004). Simoneit et al. (2004b) have documented during the ACE-
113 Asia campaign that OA from the BB and fossil fuel combustion sources are transported along
114 with desert dust to the KCOG during continental outflow. An intensive campaign was
115 organized at the KCOG during spring 2005 to observe the physical properties of East Asian
116 aerosols while two dust events were detected (Nakajima et al., 2007). Here, we focus on the
117 characterization of airborne anhydrosugars, primary sugars, sugar alcohols, and BSOA
118 tracers from the KCOG. Gosan is influenced by the continental outflow from East Asia
119 during winter, spring and fall, whereas the site is influenced by the maritime air masses from
120 the Pacific Ocean and other marginal seas during summer. This makes the KCOG ideal for
121 characterizing the regional heterogeneities in the emissions of organic compounds in the East
122 Asian outflow based on the total suspended particulate (TSP) samples collected during April
123 2013-April 2014.

124 **2. Methods**

125 **2.1. Aerosol sampling and prevailing meteorology**

126 TSP samples were collected on pre-combusted (450°C for 6 h) quartz fiber filters (20 cm ×
127 25 cm, Pallflex) at the KCOG (33.17 °N, 126.10 °E, see Figure 1), South Korea. To get
128 enough signal for the radiocarbon measurements, each TSP sample was collected for 10–14
129 days from April 2013 to April 2014. Twenty-one samples were collected using a high-volume
130 air sampler (Kimoto AS-810, ~65 m³ h⁻¹) installed on the rooftop of a trailer house (~3 m
131 above the ground). After the collection, the aerosol filters were transferred to a pre-

132 combusted (450°C for 6 h) glass jar (150 mL) equipped with a Teflon-lined screw cap and
 133 transported to the laboratory in Sapporo. These TSP samples were stored in a dark freezer
 134 room at -20°C until the analysis. Three field blank filters were also collected during the
 135 campaign.

136 The ambient temperatures at the Gosan site were on average 6.9°C in winter, 14.1°C
 137 in spring, 27.0°C in summer, and 17.1°C in fall. Likewise, the average relative humidity was
 138 found to be highest in summer (71.3%), followed by spring (64.9%), fall (63.5%), and winter
 139 (54.7%). Gosan is influenced by the pollution sources in East Asia during winter as well as
 140 other transition periods (spring and fall) due to the prevailing westerlies. In contrast, winds in
 141 summer blew mostly from the western North Pacific (WNP) by the easterly winds. The
 142 spring season is, in particular, important for the transport of mineral dust mixed with polluted
 143 OA to Gosan (Kundu et al., 2010).

144
 145

146

147

148

149

150

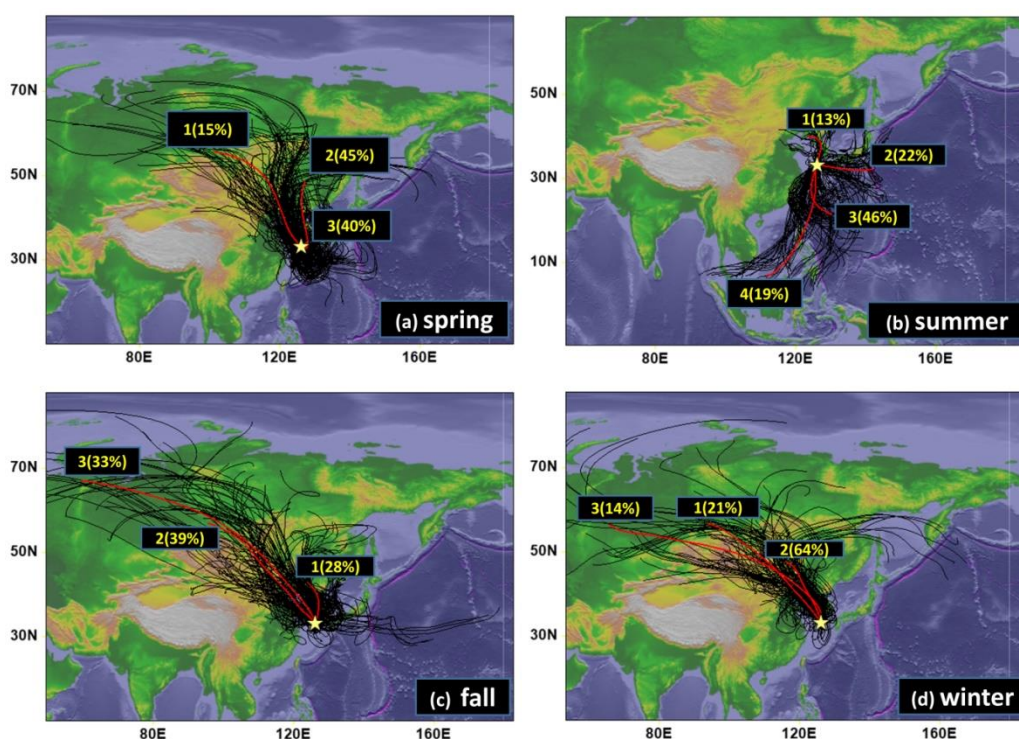
151

152

153

154

155



156 **Figure 1.** Cluster analysis of backward air mass trajectories over Gosan (indicated by a star
 157 symbol) for the TSP collected during (a) spring, (b) summer, (c) fall, and (d) winter seasons.

158

159 2.2. Extraction and analysis of organic compounds

160 Approximately 3.14 cm² filter cuts were extracted with dichloromethane/methanol (2:1; v/v).

161 The extracts were concentrated using a rotary evaporator under vacuum and then blown down

162 to near dryness with pure nitrogen gas. The dried residues were subsequently reacted with N,
163 O-bis(trimethylsilyl)trifluoroacetamide containing 1% trimethylchlorosilane (BSTFA+1%
164 TMCS, SUPELCO[®], Sigma-Aldrich[®]) and pyridine at 70 °C for 3 h to derive OH and COOH
165 groups of polar organic compounds to trimethylsilyl ethers and esters, respectively. After the
166 derivatization followed by the addition of a known amount of internal standard solution
167 (Tridecane; 1.43 ng L⁻¹ in n-hexane), the derivatized extracts were injected onto a gas
168 chromatograph (Hewlett-Packard model 6890 GC) coupled to a mass spectrometer (Hewlett-
169 Packard model 5973, MSD) (GC-MS). More details on the quantification of polar organic
170 compounds using GC-MS are described in Haque et al. (2019).

171 The target compounds (anhydrosugars, primary sugars, sugar alcohols, and BSOA
172 tracers) were separated on a DB-5MS fused silica capillary column (30 m x 0.25 mm i.d., 0.5
173 µm film thickness) using helium as a carrier gas at a flow rate of 1.0 ml min⁻¹. The GC oven
174 temperature was programmed from 50°C for 2 min and then increased from 50 to 120°C at
175 30°C min⁻¹ and to 300°C at 6°C min⁻¹ with a final isotherm hold at 300°C for 16 min. The
176 sample was injected in a splitless mode with the injector temperature at 280°C. The MS was
177 operated at 70 eV and scanned from 50 to 650 Da on an electron impact (EI) mode. Mass
178 spectral data were acquired and processed using the Chemstation software. The organic
179 compounds were identified individually by comparison with retention times and mass spectra
180 of authentic standards and NIST library and literature data of mass fragmentation patterns
181 (Medeiros and Simoneit, 2007). For assessing the recoveries, ~100-200 ng of the standard
182 solution was spiked on the blank filter and analyzed as a real sample. Overall, the average
183 recoveries were found to be 80-104% for target compounds. The field and laboratory blank
184 filters (n = 3) were also analyzed by the same procedures as a real sample. Target compounds
185 were not found in the field blanks. The analytical errors based on concentrations by replicate
186 sample analyses (n = 3) were less than 15%.

187 **2.3. Carbon fractions analysis**

188 Organic carbon (OC) and elemental carbon (EC) were analyzed using a thermal-optical
189 transmittance method with a Sunset Laboratory carbon analyzer following the NIOSH
190 protocol (Birch and Cary, 1996), and detailed procedures were given elsewhere (Zhang et al.,
191 2016). Furthermore, a portion of 2.54 cm² of each sample filter was extracted with 15 mL
192 ultrapure water (resistivity > 18.2 MΩcm, Sartorius arium 611 UV) with ultrasonication for
193 30 min. The water extracts were then filtered through a membrane disc filter for water-
194 soluble organic carbon (WSOC) analysis by a total organic carbon (TOC) analyzer

195 (Shimadzu, TOC-Vcsh) (Boreddy et al., 2018). The concentrations of WSOC were corrected
 196 by field blanks. The analytical errors in the triplicate analyses were less than 5% for WSOC.

197 **2.4. Radiocarbon isotopic composition of total carbon (TC) and EC**

198 The concentrations of TC in the TSP samples were determined using an elemental analyzer.
 199 For the radiocarbon isotopic composition ($\Delta^{14}\text{C}$), the aerosol filter punches (1.5 cm^2) were
 200 exposed for ~ 12 h to HCl fumes in a vacuum desiccator. Subsequently, the punches were
 201 analyzed for $\Delta^{14}\text{C}$ on a modified elemental analyzer coupled via a gas interface to Accelerator
 202 Mass Spectrometer Mini Carbon Dating System (MICADAS) at the University of Bern,
 203 Switzerland (Salazar et al., 2015). The evolved CO_2 of TC from the elemental analyzer was
 204 passed through a moisture trap (Sicapent, Merck) and isolated from other residual gasses
 205 using a temperature-controlled zeolite trap. The purified CO_2 was introduced through a gas
 206 interface system to MICADAS, where $^{14}\text{C}/^{12}\text{C}$ ratios are measured according to the analytical
 207 procedures detailed in Zhang et al. (2016). Likewise, the evolved CO_2 of elemental carbon
 208 from the Sunset Lab OC/EC analyzer using the Swiss 4S protocol (Zhang et al., 2012), was
 209 directed to the MICADAS and measured for the $^{14}\text{C}/^{12}\text{C}$ ratio relative to standard calibration
 210 gas. These results were expressed as fractions of modern carbon (f_{M}) by normalizing with a
 211 $\delta^{13}\text{C}$ value of the reference standard in the year 1950 (-25‰) according to Stuiver and Polach
 212 (1997) for the fractionation effects. The $f_{\text{M}}(\text{OC})$ can be estimated by using the $f_{\text{M}}(\text{TC})$ and
 213 $f_{\text{M}}(\text{EC})$ in an isotope mass balance equation (Zhang et al., 2015). Additionally, we estimated
 214 the relative contributions of OC and EC from the nonfossil and fossil sources ($f_{\text{nonfossil}}$ and
 215 f_{fossil} , respectively) using the following equations.

$$216 \quad f_{\text{nonfossil-OC}} = f_{\text{M}}(\text{OC-sample})/f_{\text{M}}(\text{OC-ref}); f_{\text{M}}(\text{OC-ref}) \approx 1.07 \pm 0.04 \quad (1)$$

$$217 \quad f_{\text{nonfossil-EC}} = f_{\text{M}}(\text{EC-sample})/f_{\text{M}}(\text{EC-ref}); f_{\text{M}}(\text{EC-ref}) \approx 1.10 \pm 0.05 \quad (2)$$

$$218 \quad f_{\text{fossil-OC}} = 1 - f_{\text{nonfossil-OC}} \quad (3)$$

$$219 \quad f_{\text{fossil-EC}} = 1 - f_{\text{nonfossil-EC}} \quad (4)$$

220 The reference values of OC and EC were obtained from Mohn et al. (2008). Using
 221 the fractions of $f_{\text{fossil-OC}}$ and $f_{\text{nonfossil-OC}}$, we can, therefore, estimate the mass concentration of
 222 ambient organic carbon (OC-ambient) from fossil and nonfossil sources ($\text{OC}_{\text{fossil}}$ and
 223 $\text{OC}_{\text{nonfossil}}$, respectively).

$$224 \quad \text{OC}_{\text{nonfossil}} = f_{\text{nonfossil-OC}} \times [\text{OC}]_{\text{ambient}} \quad (5)$$

$$225 \quad \text{OC}_{\text{fossil}} = f_{\text{fossil-OC}} \times [\text{OC}]_{\text{ambient}} \quad (6)$$

226 More details on the radiocarbon isotopic composition data over Gosan were reported
 227 elsewhere (Zhang et al., 2016).

228 3. Results and discussion

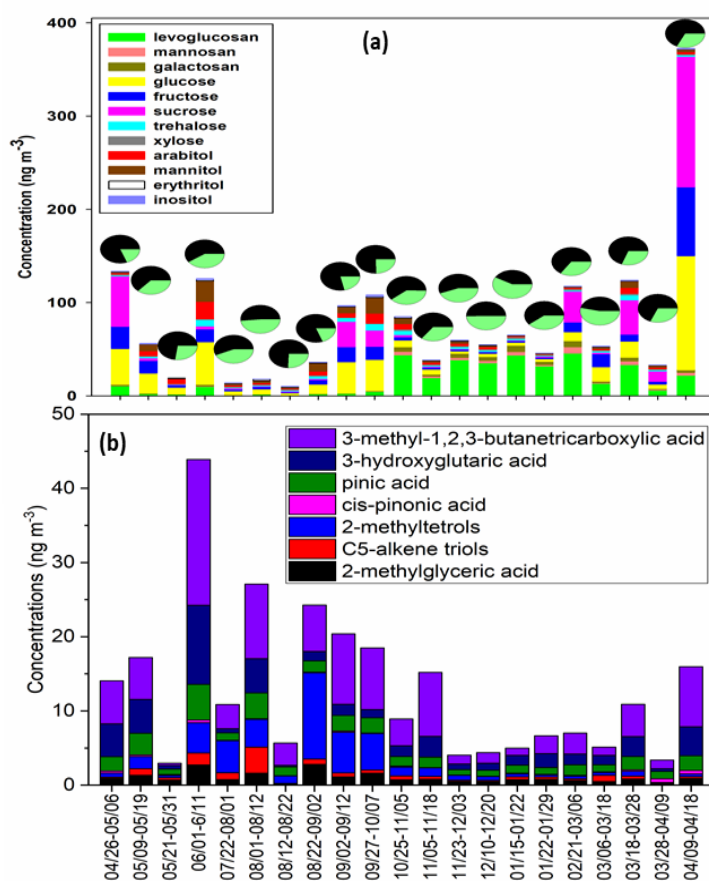
229 3.1. Trajectory and cluster analysis

230 Backward air mass trajectories are useful for assessing the impact of local versus regional
231 source emissions over Gosan. Seven-day isentropic backward air mass trajectories were
232 computed using the hybrid single-particle Lagrangian integrated trajectory model (HYSPLIT,
233 version 4: Stein et al., 2015) over the KCOG for the sampling period using the
234 meteorological datasets of the Global Data Assimilation System (GDAS) network. The
235 trajectory endpoint files from the HYSPLIT model were further used for the cluster analysis
236 using the Trajstat package (Wang et al., 2009b) for all four seasons (Figure 1). Although
237 cluster analysis revealed the predominance of continental transport in the spring, fall, and
238 winter seasons, the air masses over the KCOG in summer mostly originated from the WNP.
239 Since spring is a transition of winds switching from westerlies to easterlies, Gosan is likely
240 influenced by the long-range transport of dust, pollution, and sea-salt aerosols.

241 The vertical mixing of pollutants within the boundary layer height also plays an
242 important role in controlling the strength of continental outflow alongside regional
243 meteorology. For instance, the mixing height of air parcels from the HYSPLIT model is
244 mostly confined to 1000 m in winter but somewhat increased towards the spring and fall
245 seasons (Figure S1). This vertical enhancement in the boundary layer height facilitates the
246 transport of mineral dust particles from the arid and semiarid regions in East Asia along with
247 urban pollutants to Gosan in spring and fall compared to winter. However, the strength of the
248 continental outflow somewhat depends on several factors, including source emissions,
249 meteorology, and mixing height of air parcels.

250 Gosan is influenced by three types of air masses in spring (Figure 1a), from the
251 Mongolian Desert (cluster 1: 15%), North China (cluster 2: 45%), and from the Yellow Sea
252 (cluster 3: 40%). In contrast, the easterlies from the WNP in summer mostly influenced the
253 composition of TSP over the KCOG. This inference is based on the cluster analysis for
254 summer samples (Figure 1b), which showed four regimes, including transport from the Sea of
255 Japan (cluster 1: 13%), WNP (cluster 2: 22%), South China Sea (cluster 3: 46%), and East
256 China Sea (cluster 4: 19%). In contrast, cluster analysis revealed three major transport
257 regimes from East Asia in fall and winter (Figure 1c-d). However, there are subtle differences
258 that exist between winter and fall in terms of influence from nearby versus distant pollution
259 sources. For instance, long-range transport of air masses from west Mongolia (cluster 1:
260 21%) and the Russian Far East (cluster 3: 14%) exerted a weak influence on the TSP sampled
261 over Gosan in winter. Besides, we observed a somewhat larger impact of air masses from the

262 North China Plain over Gosan (cluster 2: 64%) in winter. In contrast, Gosan is less influenced
 263 by air masses originating from the North China Plain, contributing ~28% (cluster 1) than
 264 those from Mongolia (cluster 2: 39%) and the Russian Far East (cluster 3: 33%) in fall.
 265 Therefore, the impact of East Asian outflow is stronger in winter than in spring and fall.
 266
 267



268
 269 **Figure 2.** (a) Cumulative concentration levels of anhydrosugars, primary sugars, and sugar
 270 alcohols (i.e., represented by bars), and depicting the contributions of nonfossil (green color)
 271 and fossil (black color) organic carbon (i.e., pie charts), (b) Cumulative concentration levels
 272 of isoprene- and monoterpene-SOA tracers in each TSP sample collected over Gosan.

273

274 3.2. Temporal and seasonal variability of sugars

275 The temporal/seasonal trends of sugar compounds over the KCOG provide useful
 276 information on the emission strengths of various sources in the East Asian outflow. All three
 277 anhydrosugars showed similar temporal and seasonal trends with higher concentrations in
 278 winter and fall than spring and summer (Figures 2a and S2). As levoglucosan and two other
 279 anhydrosugars (mannosan and galactosan) are the pyrolysis products of

280 cellulose/hemicellulose, their higher concentrations along with an increase in nonfossil
281 fraction of OC (Figure 2a; pie charts) in TSP from winter and fall revealed the impact of BB
282 emissions. The MODIS satellite-based fire counts (Figure S1) together with cluster analysis
283 in winter and fall (Figure 1) have revealed an influence of active BB emissions in the North
284 China Plain, Mongolia, and the Russian Far East. The temporal trends of glucose, fructose,
285 and sucrose exhibited less variability throughout the sampling period; however, we observed
286 a slight increase in their concentration towards spring/summer (Figure 2a). Glucose and
287 fructose have origins from leaf fragments and pollen species (Fu et al., 2012a). Sucrose is a
288 potential tracer for airborne pollen (Fu et al., 2012a) and late spring/early summer is often
289 regarded as a season of “pollen-allergies”. Therefore, the similar temporal trends of glucose
290 and fructose with sucrose indicate their common source, pollens (Figure 2a). Since glucose,
291 fructose, and sucrose showed moderately significant correlations ($R^2 = 0.44-0.48$, $p < 0.01$)
292 with levoglucosan in winter, it is somewhat possible that BB source emission could also
293 influence the concentrations of these saccharides in this season (Haque et al., 2019; Fu et al.,
294 2008).

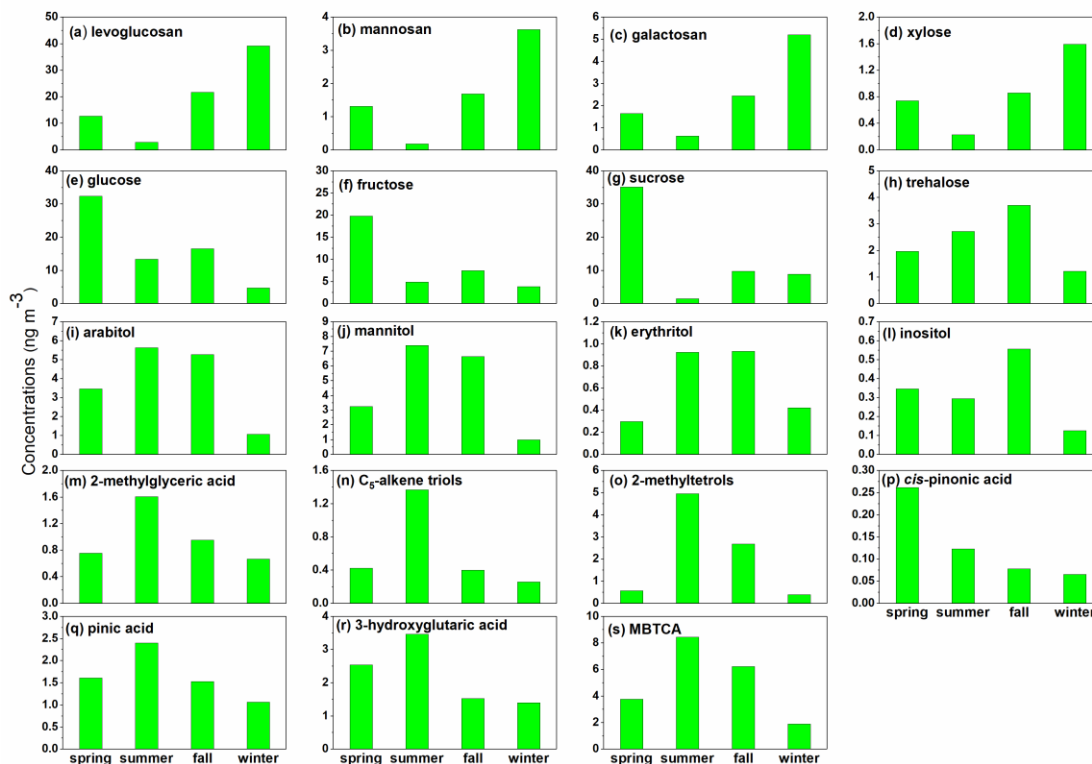
295 BB also contributes to xylose and, hence, the temporal variability of xylose is
296 mimicking that of the anhydrosugars. Trehalose is a primary sugar and a useful tracer for
297 organic carbon associated with soil dust particles (Fu et al., 2012a). The temporal variability
298 of trehalose closely resembles that of the fungal spore tracers (arabitol, mannitol, and
299 erythritol), showing high concentrations in the spring, summer, and fall seasons (Figures 2a
300 and S2) (Zhu et al., 2015a; Fu et al., 2012a). The KCOG is under the influence of a large-
301 scale advection of mineral dust from East Asia to the WNP during these three seasons (Tyagi
302 et al., 2017; Huebert et al., 2003). The mineral dust transport from East Asia to the WNP can
303 be traced by the high concentrations of non-sea-salt Ca^{2+} in the TSP samples from Gosan
304 (Arimoto et al., 1996). Similar temporal trends of trehalose and nss- Ca^{2+} , particularly in
305 spring samples (Figure S3), suggest that the abundance of OA specific to fungal spores over
306 Gosan is likely associated with the Kosa (Asian dust) events.

307 The major sources of arabitol and mannitol are airborne fungal spores (Bauer et al.,
308 2008), accompanying detritus from mature leaves (Pashynska et al., 2002). Heald and
309 Spracklen (2009) reported that mannitol and arabitol are considerably associated with
310 terrestrial biosphere activity. Inositol is largely derived from the developing leaves in summer
311 (Pashynska et al., 2002) and BB in winter (Fu et al., 2010b). Zhu et al. (2015b) found a
312 similar seasonal behavior of inositol with those of other sugar alcohols with the
313 predominance in summer, associated with microbial activities in local forests from Okinawa.

314 Inositol showed a moderately significant correlation with levoglucosan ($R^2 = 0.33$, $p < 0.01$)
315 in winter; however, there were no positive linear relationships between levoglucosan and
316 other sugar alcohols, implying a partial emission of inositol from the BB during winter in
317 Gosan aerosols. Therefore, the temporal variability of inositol differs from that of the other
318 sugar alcohols (Figure S2). The sources of sugar compounds are further discussed in section
319 3.4.

320 The seasonally averaged concentrations of all the anhydrosugars and xylose are
321 higher in winter/fall than spring/summer (Figure 3a-d), possibly due to a greater influence of
322 long-range transport from East Asia. In contrast, glucose, fructose, and sucrose peaked in
323 spring but decreased in the other seasons (Figure 3e-g), mainly because of the contribution of
324 airborne pollen. Trehalose showed higher concentrations in fall and summer, followed by
325 spring and winter (Figure 3h). Arabitol, mannitol, and erythritol showed higher
326 concentrations in summer/fall than in winter and spring (Figure 3i-k). This seasonal trend is
327 consistent with those of soil-derived fungal spores. This feature is consistent with earlier
328 observations from a remote oceanic island in the WNP (Okinawa) during the impact of East
329 Asian outflow (Zhu et al., 2015a). The seasonally averaged mass concentrations of inositol
330 are highest in spring, followed by summer, fall, and winter (Figure 3l). Overall, the molecular
331 compositions of anhydrosugars showed the predominance of levoglucosan followed by
332 galactosan and mannosan (Figure S4). Galactosan is more abundant in crop-residue burning
333 emissions than mannosan (Engling et al., 2009; Sheesley et al., 2003). It is very much likely
334 that the impact of crop-residue burning emissions in East Asia over Gosan is more prominent
335 in winter/spring. Such high abundances of galactosan over mannosan were found in the North
336 China Plain (Fu et al., 2008) and in the Indo-Gangetic Plain outflow sampled over the Bay of
337 Bengal (Bikkina et al., 2019). Although the temporal variability of primary sugars in the TSP
338 samples from Gosan showed a characteristic peak of glucose and sucrose (Figure 2a), the
339 seasonally averaged distributions are different (Figure S4). The molecular distributions of
340 sugar alcohols are characterized by high loadings of arabitol and mannitol, followed by
341 erythritol and inositol (Figure S4).

342



343

344 **Figure 3.** Seasonal variability of the atmospheric levels of sugar compounds and BSOA
 345 tracers in TSP samples from Gosan during April 2013-April 2014.

346

347 3.3. Temporal and seasonal variability of BSOA tracers

348 We identified six isoprene-SOA tracers such as 2-methylglyceric acid (2-MGA), three C₅-
 349 alkene triols, and two 2-methyltetrols (2-methylthreitol and 2-methylerythritol) (2-MTs) in
 350 Gosan aerosol samples (Table 1). The sum of the isoprene-SOA tracers ranged from 0.35 to
 351 15.1 ng m⁻³ (avg. 3.69 ng m⁻³) with the predominance of 2-MTs (avg. 2.09 ng m⁻³). 2-MGA is
 352 the second most abundant isoprene-SOA tracer (avg. 0.99 ng m⁻³), a high-generation product
 353 probably formed by further photooxidation of methacrolein and methacrylic acid. A similar
 354 molecular composition was observed over the North Pacific and California Coast (Fu et al.,
 355 2011). All the isoprene-SOA tracers exhibited similar temporal variations with higher
 356 concentrations in the summer/spring months compared to autumn and winter (Figure 2b).
 357 Conversely, four monoterpene-SOA tracers, i.e., *cis*-pinonic acid, pinic acid, 3-
 358 hydroxyglutaric acid (3-HGA), and 3-methyl-1,2,3-butanetricarboxylic acid (MBTCA), were
 359 detected in the Gosan samples (Table 1). The total concentrations of monoterpene-SOA
 360 tracers were found to be 1.65 to 35.5 ng m⁻³ (avg. 9.24 ng m⁻³) with a high concentration of
 361 MBTCA (avg. 5.11 ng m⁻³). All the monoterpene-SOA tracers showed similar temporal
 362 trends with high values in summer/spring periods than autumn/winter (Figure 2b).

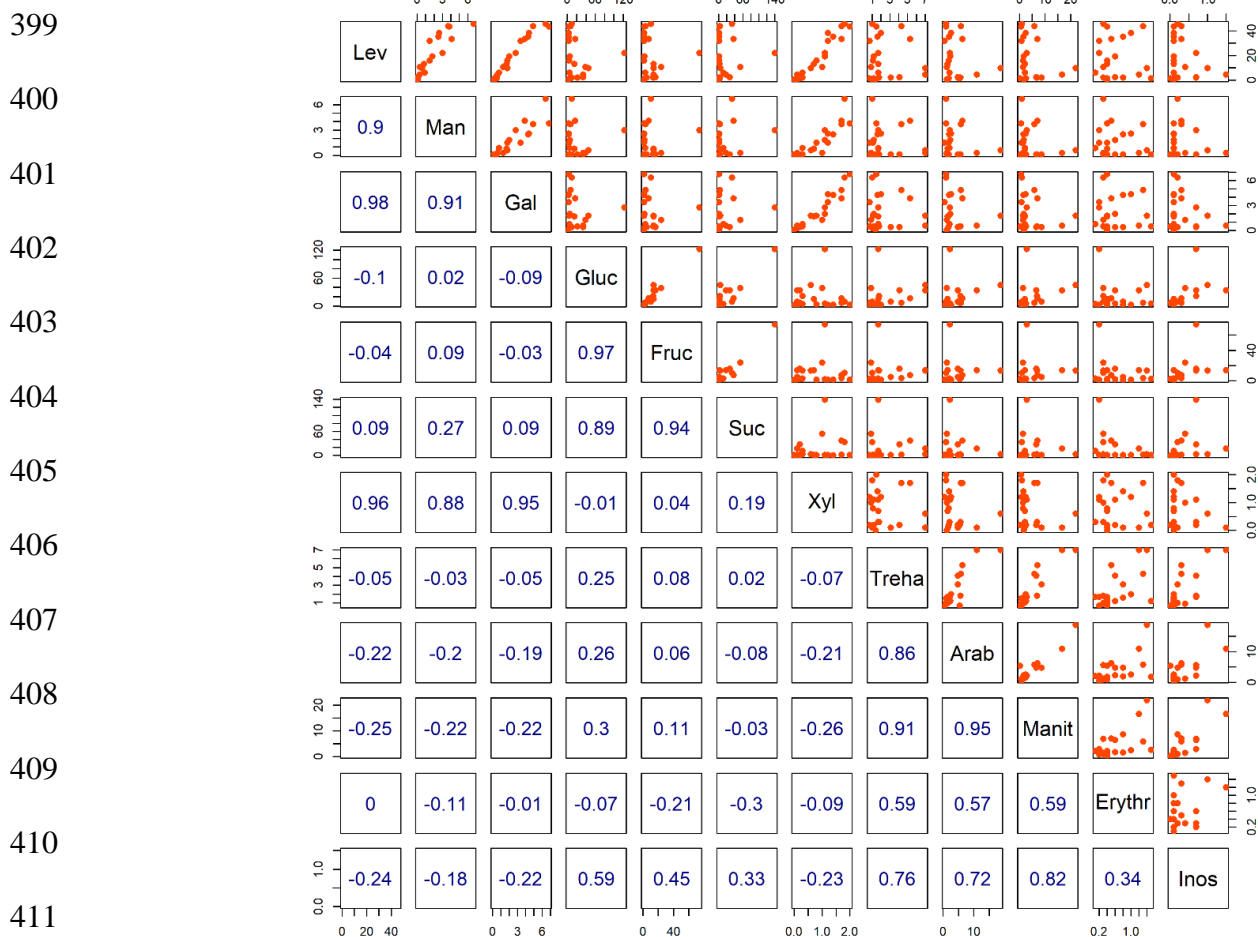
363 Nevertheless, *cis*-pinonic acid exhibited a somewhat different temporal variability than the
364 other monoterpene-SOA tracers. It is likely that *cis*-pinonic acid might be further photo-
365 oxidized to form MBTCA (Szmigielski et al., 2007).

366 The seasonal average of isoprene-SOA tracers showed high concentrations in
367 summer, followed by spring/fall and winter (Figure 3m-o). One key feature of the data
368 presented here is that two fall samples (KOS984; 2-12 September and KOS986; 27
369 September to 07 October) exhibited high concentrations for 2-MTs over Gosan (Figure 2b).
370 We presumed that local vegetation might contribute significantly to the formation of 2-MTs
371 as they are first-generation products. Moreover, 2-MTs can be derived from the open ocean
372 under low NO_x conditions (Hu et al., 2013). 3-HGA and pinic acid showed somewhat higher
373 concentrations in summer/spring than fall/winter due to the growing vegetation (Figure 3q-r).
374 *Cis*-pinonic acid was more abundant in spring compared to summer (Figure 3p) because of its
375 photo-degradation, as discussed above. In contrast, MBTCA was more dominant in
376 summer/fall than in spring/winter (Figure 3s). Here, the formation of MBTCA could be
377 enhanced in fall during atmospheric transport from East Asia. The molecular distributions of
378 isoprene-SOA tracers were characterized by a high loading of 2-MTs, followed by 2-MGA
379 and C₅-alkene triols in all seasons (Figure S4). The molecular composition of monoterpene-
380 SOA tracers was dominated by MBTCA, followed by 3-HGA, pinic acid, and *cis*-pinonic
381 acid in all seasons (Figure S4). Overall, BSOA tracers were found to be most abundant in
382 summer, followed by fall, spring, and winter (Table 1). Interestingly, it is likely that
383 secondary OA undergoes much faster cycling than the primary sugar compounds, considering
384 the feasibility of photooxidation. This would mean a slight underestimation of BSOA over
385 the KCOG in the East Asian outflow and, hence, their atmospheric abundances over Gosan
386 reflect a lower limit.

387 Kang et al. (2018b) reported that monoterpene-SOA tracers were more abundant than
388 isoprene-SOA tracers in spring-summer over the East China Sea, which is consistent with this
389 study. Although the mass budget calculations showed that isoprene and monoterpenes are
390 largely emitted by terrestrial plants, the open ocean can also contribute to isoprene and
391 monoterpenes significantly (Conte et al., 2020; Shaw et al., 2010; Broadgate et al., 1997). Air
392 mass back trajectory and cluster analysis (Figure 1) implied that the air masses mostly
393 originated from the ocean during summer. This means the open ocean significantly
394 contributed to isoprene-SOA production. However, terrestrial sources from the continent also
395 substantially enhanced the formation of BSOA. For example, one sample (KOS979; 1-11

396 June 2013) during summer showed the highest loading of BSOA tracers (Figure 2b) when air
 397 masses were transported from the continent (Zhang et al., 2016).

398



412 **Figure 4.** Multiple linear regression (MLR) analysis of airborne sugar compounds in TSP
 413 collected over Gosan.

414

415 3.4. Source apportionment- regression analysis and diagnostic ratios

416 The anhydrosugars strongly correlated with xylose (Figure 4), suggesting their common
 417 source as BB emission in East Asia. Fu et al. (2012a) analyzed pollen from different tree
 418 species (e.g., White birch, Chinese willow, Peking willow, Sugi, Hinoki), which are enriched
 419 in sucrose ($182\text{-}37,300 \mu\text{g g}^{-1}$), glucose ($378\text{-}3601 \mu\text{g g}^{-1}$) and fructose ($162\text{-}1813 \mu\text{g g}^{-1}$). In
 420 our samples, sucrose strongly correlated with glucose and fructose (Figure 4), suggesting
 421 their origin from plant-derived airborne pollen. Likewise, a strong correlation was found
 422 between arabitol and mannitol, indicating a mutual origin from a similar type of fungal spores
 423 (Zhu et al., 2015a; Fu et al., 2012a; Bauer et al., 2008; Yttri et al., 2007). Bauer et al. (2008)

424 ascribed weak correlations between arabitol and mannitol to the diverse nature of ambient
425 fungal spores. Furthermore, both sugar alcohols correlated well with trehalose, a tracer for
426 soil organic carbon (Fu et al., 2012a). This observation suggests their common origin from
427 soil organic matter associated with fungal spores. Erythritol also originates from fungal
428 spores; however, its abundance is affected by the atmospheric aging process. Kessler et al.
429 (2010) reported that erythritol is degraded during long-range transport in 12.7 days.
430 Consequently, arabitol and mannitol were moderately correlated with erythritol in the Gosan
431 samples due to the degradation of the latter sugar alcohol in the East Asian outflow.

432 The linear relationship of levoglucosan (*Lev*) with mannosan (*Man*), galactosan (*Gal*),
433 and nss-K^+ provides useful information on the type of BB emissions (hardwood, softwood, or
434 crop-residue). Ratios of *Lev/Man* and *Lev/(Man + Gal)* can be useful to distinguish BB and
435 coal combustion contributions. The average ratios of *Lev/Man* (15.1 ± 6.76) and *Lev/(Man +*
436 *Gal)* (4.27 ± 1.23) in Gosan aerosols are much closer to those from wood burning and coal
437 combustion sources emissions, respectively (Yan et al., 2018). It reveals that *Lev* could
438 originate from both biomass and coal burning source emissions, which is consistent with the
439 linear relationship between *Lev-C* and the fossil-/nonfossil carbon fraction (section 3.6).
440 Furthermore, different types of biomass are characterized by distinct *Lev/Man* ratios. For
441 instance, *Lev/Man* ratios from the softwood burning emissions (3-10) differ from those of
442 hardwood (15-25) and crop-residues (>40) (Singh et al., 2017; Schmidl et al., 2008a, b; Fu et
443 al., 2008; Engling et al., 2006, 2009; Fine et al., 2001, 2004). We found that the *Lev/Man*
444 ratios (Table 2) over the KCOG overlap between seasons and are somewhat close to that of
445 hardwood burning emissions in northern China, Mongolia, and the Russian Far East, as
446 corroborated by the backward air mass trajectories and MODIS fire counts (Figures 1 and
447 S1). Besides, *Lev/K⁺* and *Man/Gal* ratios in summer differ from those of other seasons (Table
448 2). Cheng et al. (2013) have apportioned qualitatively the source contributions of
449 anhydrosugars over a receptor site based on the comparison of *Lev/K⁺* and *Lev/Man* ratios in
450 aerosols to those from various source profiles compiled from the literature. This approach of
451 using the mass ratios of *Lev/Man* and *Lev/K⁺* has been proven useful for deciphering the
452 difference in BB-derived OA (Bikkina et al., 2019).

453 Here, we adopted this methodology to ascertain the likely contributing sources of
454 anhydrosugars, which are BB tracers from different seasons (Figure 5). This source
455 apportionment relies on the fact that the *Lev/K⁺* ratio from the softwood burning (10-1000) is
456 higher than from hardwood (1-100) (Fine et al., 2004). In contrast, *Lev/Man* ratios for
457 softwood are lower than those of hardwood burning (10-100) (Fine et al., 2004). Likewise,

458 the Lev/Man and Lev/K^+ ratios from grasses and crop-residues are 10-100 and 0.01-1.0,
 459 respectively (Bikkina et al., 2019). On a similar note, the Lev/K^+ ratios from the burning of
 460 pine needles (0.1-1.0) somewhat overlap with those from hardwood burning emissions but
 461 are characterized by distinct Lev/Man ratios (Bikkina et al., 2019). The burning of dead
 462 leaves (duff) showed higher Lev/K^+ ratios than those of pine needles and grasses, but their
 463 Lev/Man ratio is on the lower side than for the former biomass type and the softwood burning
 464 emissions. However, Lev is more susceptible to degradation by photooxidation with OH
 465 radicals during atmospheric transport (half-life: <2.2 days) (Hennigan et al., 2010) and this
 466 would cause lower abundances of this anhydrosugar. Hence, the hardwood Lev/K^+ ratios
 467 could slightly shift downwards. Therefore, caution is required while interpreting the ambient
 468 data from a receptor site (Bikkina et al., 2019). Overlapping the seasonal data on this scatter
 469 plot of Lev/K^+ versus Lev/Man (Figure 5) clearly reveals a mixed contribution of burning of
 470 hardwood and crop-residue in the East Asian outflow. It should be noted that the
 471 photooxidation process during atmospheric transport is also applicable for low concentrations
 472 and poor correlations of other primary saccharides.

473

474

475

476

477

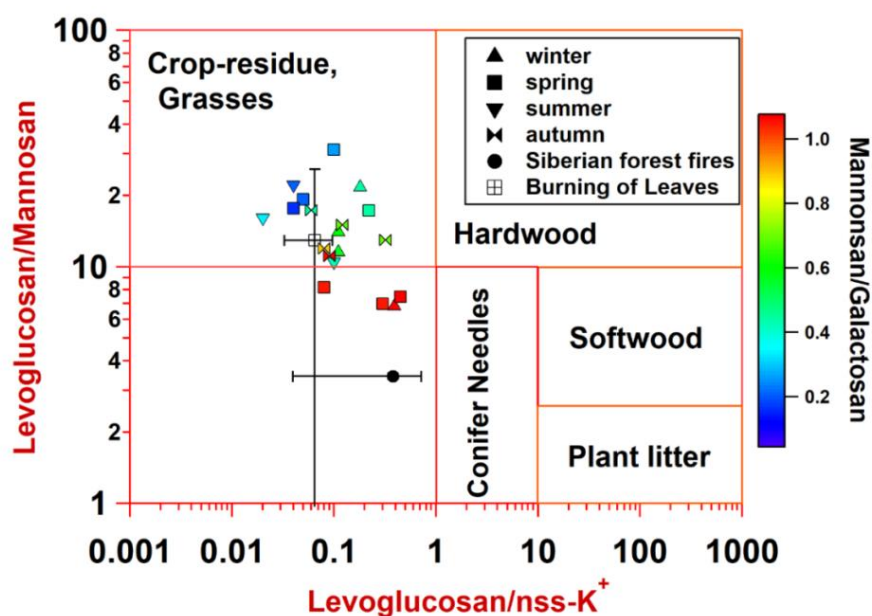
478

479

480

481

482

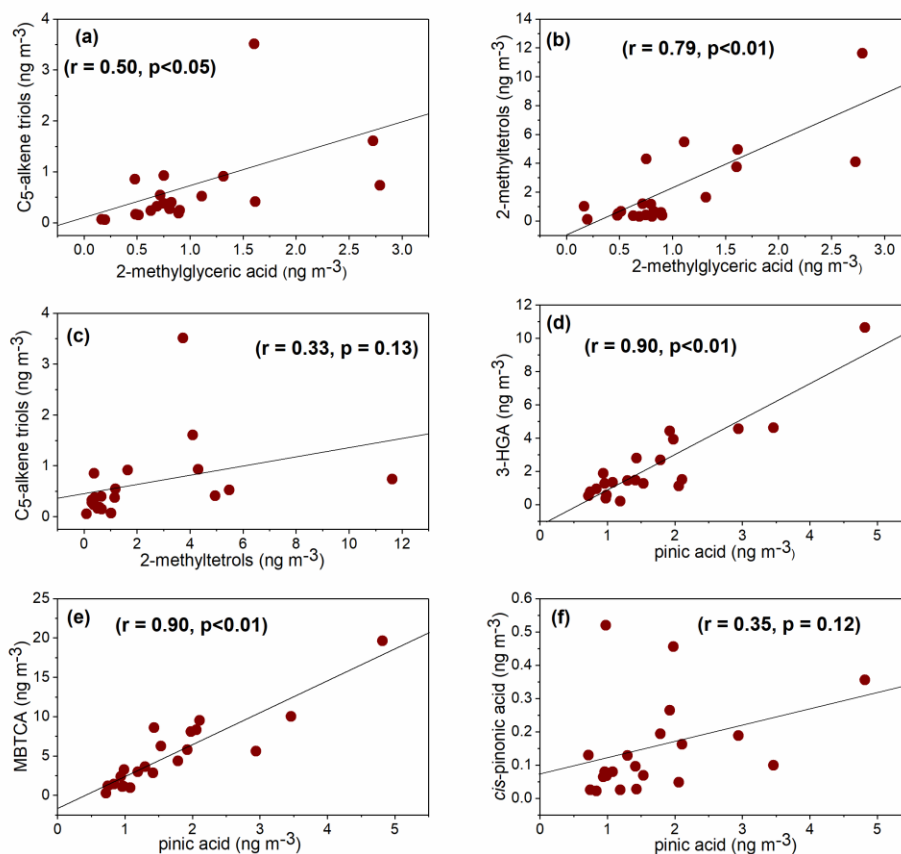


483 **Figure 5.** Scatter plot of levoglucosan/ K^+ versus levoglucosan/mannosan ratios in TSP
 484 collected over Gosan during April 2013-April 2014. The data for Siberian forest fires and
 485 burning leaves were adopted from Sullivan et al. (2008).

486

487 The correlation coefficients and diagnostic ratios of BSOA tracers specify their source
488 origin or formation pathway. Nevertheless, atmospheric stability or reactivity of BSOA
489 tracers through the photooxidation during long-range transport may bias the correlation
490 coefficients in Gosan aerosols. 2-MGA showed a significant correlation with 2-MTs ($r =$
491 0.79 , $p < 0.01$) and C_5 -alkene triols ($r = 0.50$, $p < 0.05$) (Figure 6a-b), suggesting their similar
492 formation pathway or common sources of isoprene-SOA tracers. However, a poor correlation
493 coefficient between 2-MTs and C_5 -alkene triols ($r = 0.33$, $p = 0.13$) (Figure 6c) indicates their
494 different formation process over the Gosan atmosphere. Wang et al. (2005) documented that
495 polyols are formed from isoprene through diepoxy derivatives, which further convert into 2-
496 MTs by acid-catalyzed hydrolysis. On the other hand, C_5 -alkene triols are produced from the
497 precursor of hydroxyperoxy radicals that are initially derived from isoprene through
498 rearrangement reactions (Surratt et al., 2006). It can be noted that the formation mechanisms
499 of 2-MGA and 2-MTs are different while depending on the NO_x concentrations (Surratt et al.,
500 2010). Thus, the ratio of 2-MGA/2-MTs attributes to the influence of NO_x on isoprene-SOA
501 formation. We found a low ratio of 2-MGA/2-MTs (0.67) (Figure S5a, Table 2) in summer,
502 implying enhancement of 2-MTs formation over the open ocean due to the low- NO_x
503 environment in the ocean atmosphere. On the contrary, the 2-MGA/2-MTs ratios for other
504 seasons were >1.0 (Figure S5a, Table 2), indicating an elevated formation of 2-MGA through
505 continental high NO_x condition, which is consistent with the air masses back trajectory.

506



507

508 **Figure 6.** Pearson linear correlation coefficient analysis of BSOA tracers in Gosan TSP
 509 aerosols during April 2013-April 2014.

510

511 *Cis*-pinonic acid showed a weak correlation with pinic acid ($r = 0.35$, $p = 0.12$)
 512 (Figure 6f), suggesting that different atmospheric reactivity of *cis*-pinonic/pinic acids during
 513 transport would cause such poor correlation. In contrast, pinic acid exhibited a strong positive
 514 linear correlation with 3-HGA ($r = 0.90$, $p < 0.01$) and MBTCA ($r = 0.90$, $p < 0.01$) (Figure 6d-e),
 515 implying their similar sources. It should be noted that the formation processes of pinic acid,
 516 3-HGA, and MBTCA are different because pinic acid is a first-generation product, and 3-
 517 HGA and MBTCA are high-generation products (Claeys et al., 2007; Müller et al., 2012;
 518 Szmigielski et al., 2007). The ratio of *cis*-pinonic acid + pinic acid to MBTCA (P/M) is used
 519 to evaluate the aging of monoterpene-SOA.

520 A low P/M ratio suggests the transformation of *cis*-pinonic and pinic acids to
 521 MBTCA and thus relatively aged monoterpene-SOA, whereas a high ratio reflects relatively
 522 fresh monoterpene-SOA (Gómez-González et al., 2012; Ding et al., 2014). Gómez-González
 523 et al. (2012) reported aged monoterpene-SOA (P/M = 0.84) from a Belgian forest site while
 524 fresh chamber-produced α -pinene-SOA tracers showed P/M ratios of 1.51 to 3.21 (Offenberg

525 et al., 2007). The average ratio of P/M in this study was 0.62 with the low value in summer
526 (Figure S5b, Table 2), which is lower than those of Guangzhou (fresh monoterpene-SOA;
527 28.9) while the air masses originated from southern China (Ding et al., 2014). This
528 observation indicates that monoterpenes SOA have undergone substantial aging during
529 transport to Gosan, particularly in summer when extensive photochemical oxidation occurred
530 due to the high temperature and intense solar radiation.

531 **3.5. Relative abundances in WSOC and OC**

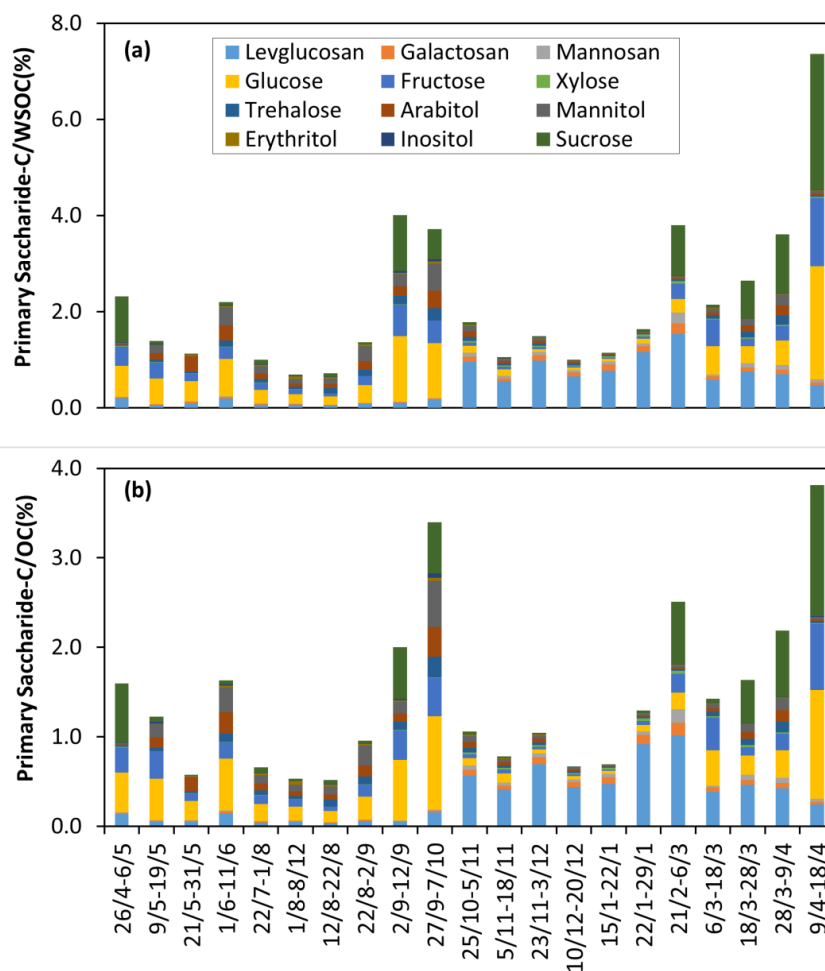
532 Levoglucosan is the most abundant anhydrosugar, contributing 0.05-1.54% of WSOC and
533 0.03-1.02% of OC. Likewise, sucrose, glucose, and fructose were more abundant primary
534 sugars, contributing 0.01-2.83%, 0.03-1.22%, and 0.02-0.74% of WSOC, respectively.
535 Contributions of the three primary sugars varied from 0.05% to 3.41% of OC. Arabitol and
536 mannitol are the most abundant sugar alcohols, whose contribution to WSOC and OC ranged
537 from 0.02% to 0.93% and 0.01% to 0.85%, respectively. Figure 7 depicts the contribution of
538 sugar compounds to WSOC and OC in TSP collected over Gosan during the study period.
539 We also compared the atmospheric abundances of sugar compounds from Gosan with the
540 literature data (Table 3). This comparison revealed the less influence of BB tracer compounds
541 (i.e., anhydrosugar levels) over Gosan, a factor of 5-10 times lower than those reported for
542 the BB-influenced source regions in China and East Asia (Fu et al., 2012b; Kang et al.,
543 2018a; Wang and Kawamura, 2005; Wang et al., 2012). However, the levels of anhydrosugar
544 over Gosan are higher than those observed over the remote Canadian High Arctic site (Fu et
545 al., 2009a). In contrast, Gosan is characterized by high concentrations of primary sugars
546 compared to other remote sampling sites in Table 3. This is because of the overwhelming
547 contribution of primary sugars associated with soil dust particles over Gosan during the East
548 Asian outflow. Such high loadings of primary sugars were observed from other remote island
549 receptor sites in the WNP (Okinawa) during the spring season (Zhu et al., 2015a). Likewise,
550 the concentrations of sugar alcohols from Gosan are similar to those from other receptor sites
551 influenced by the East Asian outflow (Verma et al., 2018; Zhu et al., 2015a).

552

553

554

555



556

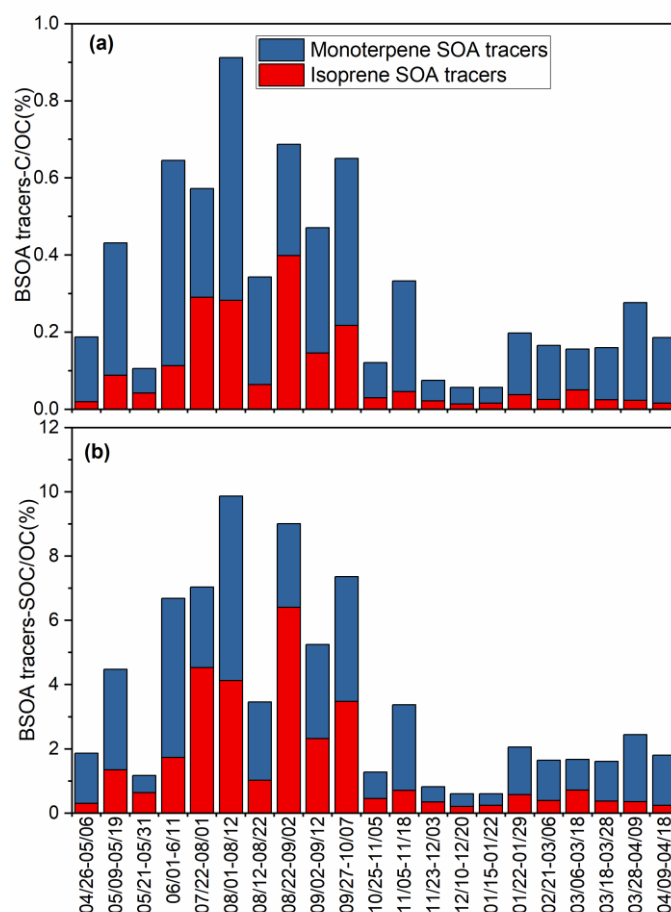
557 **Figure 7.** Contribution of primary saccharide-C in (a) WSOC(%) and (b) OC(%) in TSP
 558 collected over Gosan during April 2013-April 2014.

559

560 The contributions of isoprene-SOA tracers to ambient OC (0.01-0.40%, avg. 0.09%)
 561 and WSOC (0.02-0.57%, 0.13%) were lower than those of monoterpene-derived SOA (0.04-
 562 0.63%, 0.23% for OC and 0.06-0.82%, 0.33% for WSOC). The contributions of isoprene
 563 oxidation products to OC and WSOC were found to be highest in summer (0.23% and 0.32%,
 564 respectively), followed by fall (0.09% and 0.13%), spring (0.04% and 0.06%), and winter
 565 (0.02% and 0.03%). Likewise, the contributions of monoterpene-SOA products to aerosol OC
 566 and WSOC exhibited the highest value in summer (0.40% and 0.55%, respectively), followed
 567 by fall (0.24% and 0.35%), spring (0.18% and 0.27%), and winter (0.10% and 0.14%). We
 568 found that the contribution of BSOA products to the carbonaceous components was twice in
 569 summer (Figure 8, Table 2). This means BSOA formation occurred in summer to a greater
 570 extent due to the intensive BVOCs emission with key factors of meteorological parameters
 571 (higher temperature and radiation), i.e., higher concentrations of ozone, and other oxidizing

572 agents (NO_x , OH, etc.). It should be pointed out that the fraction of WSOC in OC
 573 (WSOC/OC) is often prone to photochemical aging and, hence, contributes to SOA. More
 574 specifically, the $\text{WSOC/OC} > 0.4$ over a receptor site indicates aged aerosols with a
 575 significant SOA contribution (Haque et al., 2019; Boreddy et al., 2018). In our study, the
 576 average WSOC/OC ratio observed was 0.68 with the highest ratio in summer (0.72), although
 577 a subtle difference existed in winter/autumn (> 0.68), implying the presence of aged OA over
 578 the KCOG. Such higher abundances of SOA over Gosan during transport from East Asia is
 579 mainly due to photochemical aging of anthropogenic (fossil fuel/biomass combustion)
 580 emissions. Huang et al. (2014) reported significant SOA formation from the fossil
 581 fuel/biomass combustion precursor VOCs in winter over China.

582



583

584 **Figure 8.** Contribution of (a) isoprene- and monoterpene-SOA tracers-C in ambient OC(%)
 585 and (b) isoprene- and monoterpene-SOA tracers-SOC in ambient OC(%) in Gosan aerosol
 586 samples during April 2013-April 2014.

587

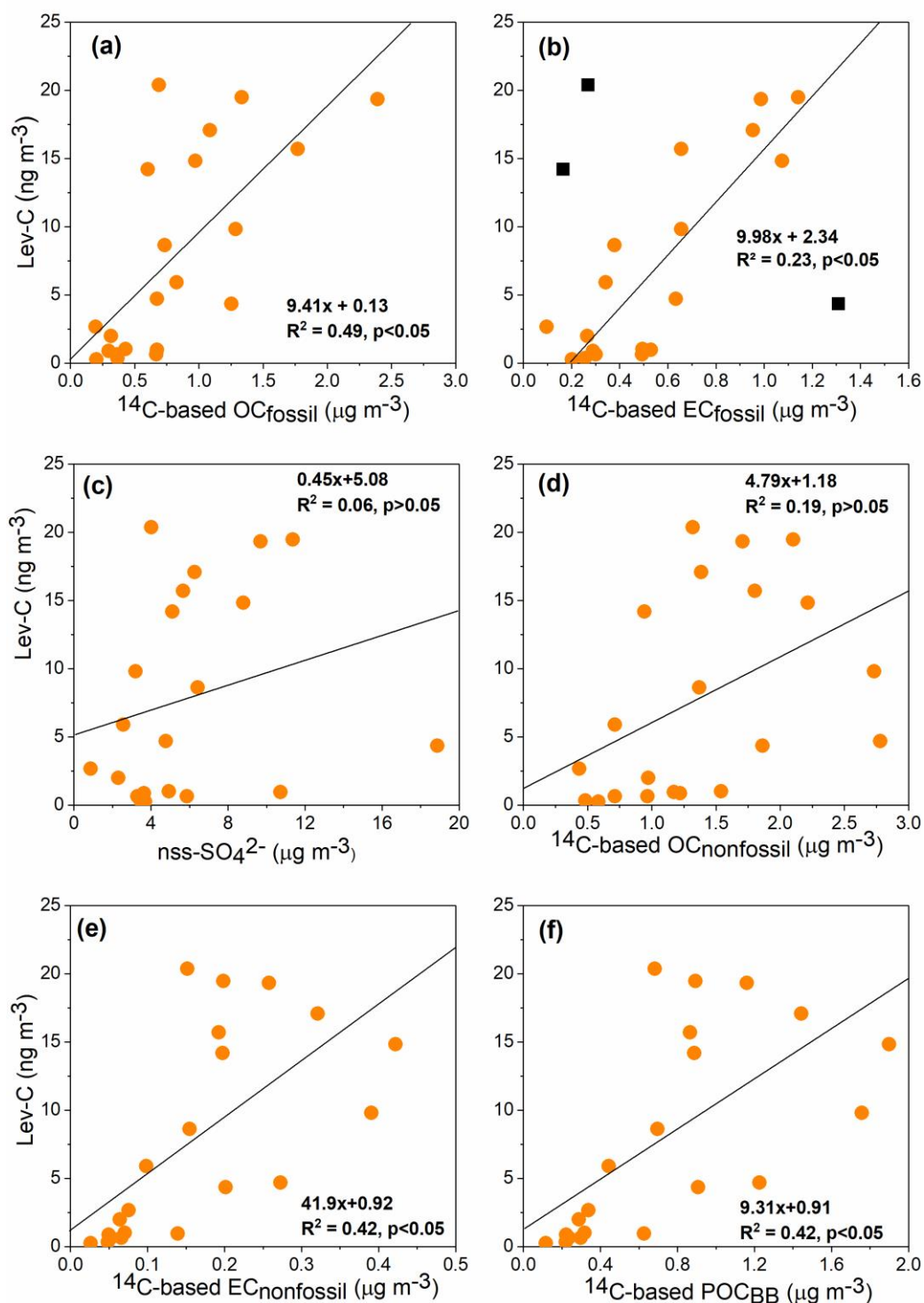
588 We estimated secondary organic carbon (SOC) derived from isoprene and
589 monoterpenes, using the measured values of BSOA tracers and following the SOA tracer-
590 based method first proposed by Kleindienst et al. (2007). A summary of the estimated SOC is
591 provided in Table 2. The contribution of isoprene to SOC was calculated 2.26 to 97.4 ngC m⁻³
592 ³ (avg. 23.7 ngC m⁻³), accounting for 1.45% of OC and 35.5% of total BSOA with the
593 predominance in summer (3.56% and 46.6% for OC and SOC, respectively). The estimation
594 of monoterpene-SOA to SOC (avg. 40.1 ngC m⁻³) was observed around two times higher than
595 that of isoprene-SOA (Table 2). Interestingly, the contribution of monoterpene-derived SOC
596 to ambient OC (3.65%) was dominant in summer, but monoterpene SOC to total SOC
597 (72.1%) was most abundant in spring (Figure 8b). The seasonal distributions of biogenic
598 SOC (Table 2) imply that a substantial amount of SOC was formed from monoterpenes in
599 spring. The estimated biogenic SOC at the KCOG is almost one order of magnitude lower
600 than that from other continental sites in Chinese urban areas (e.g., Pearl River Delta: 446 ngC
601 m⁻³) (Ding et al., 2012). However, the estimated biogenic SOC load from the KCOG is much
602 higher than that reported from a remote site in the Canadian High Arctic (Alert: 9.4 ngC m⁻³)
603 (Fu et al., 2009b) and comparable with that over the East China Sea (Kang et al., 2018b).

604 It should be noted that concentrations of SOA tracers cannot always provide the
605 actual contribution of the biogenic source to ambient organic aerosol mass. For example,
606 loadings of monoterpene-SOA tracers were lower in sample KOS999 (28 March - 9 April
607 2014) (3.02 ng m⁻³) compared to sample KOS1000 (9 - 18 April 2014) (14.4 ng m⁻³), whereas
608 the estimated contribution of SOC to ambient OC showed an opposite trend (KOS999:
609 2.08%; KOS1000: 1.56%). This result demonstrates that the estimation of SOC is an
610 important factor in evaluating the contribution of BSOA to organic aerosol mass. We
611 calculated biogenic OC using radiocarbon (¹⁴C) data following the method proposed by
612 Szidat et al. (2006). Biogenic OC showed a poor correlation with biogenic SOC ($r = 0.36$, $p =$
613 0.09) but a significant linear relationship with primary sugars (i.e., glucose, fructose and
614 sucrose) ($r = 0.54$, $p < 0.5$), suggesting that primary bioaerosols from plant-derived airborne
615 pollen dictate biogenic OC over Gosan.

616 **3.6. Significance of fossil fuel as a source for levoglucosan**

617 The ambient *Lev* levels showed a significant linear relationship with the OC_{fossil}, suggesting
618 the fossil source contribution of this molecular marker (Figure 9a). However, such a
619 significant correlation was not evident between OC_{fossil} and other major sugar compounds.
620 Until recently, *Lev* has been thought to originate primarily from the hemicellulose/cellulose
621 pyrolysis of vegetation and, hence, can be employed as a powerful tracer for biomass smoke

622 particles (Fraser and Lakshmanan, 2000; Simoneit et al., 1999). Nevertheless, residential
623 coals (e.g., lignite and bituminous coal) have been shown to contain high concentrations of
624 'Lev' but also emit traces of *Man and Gal* (Kourtchev et al., 2011; Fabbri et al., 2008).
625 Recently, Yan et al. (2018) found a significant linear relationship between the ^{14}C -based
626 fossil fraction of WSOC and *Lev-C* in the aerosols generated from coal combustion and the
627 ambient aerosol samples. Therefore, the prevailing linear relationship between $\text{OC}_{\text{fossil}}$ and
628 *Lev-C* in the Gosan samples (Figure 9a) is likely due to a common source contribution from
629 coal combustion in East Asia.



630

631 **Figure 9.** Linear regression analysis between levoglucosan in terms of its carbon content
 632 (*Lev-C*) and ¹⁴C-based mass concentrations of (a) organic carbon and (b) elemental carbon of
 633 fossil origin (OC_{fossil} and EC_{fossil}, respectively), (c) nss-SO₄²⁻, (d) nonfossil derived organic
 634 carbon (OC_{nonfossil}), (e) nonfossil derived elemental carbon (EC_{nonfossil}), and (f) biomass
 635 burning derived primary OC (POC_{BB}) in TSP collected over Gosan during April 2013-April
 636 2014. In panel (b), the squares represent three outliers (i.e., samples with rather high and low
 637 *Lev/EC* ratios; please see text for more details).

638 The slope of the linear regression between $Lev-C$ and OC_{fossil} (0.0094; Figure 9a) is
 639 higher than those documented for the coal combustion source in China ($\sim 0.004 \pm 0.007$) (Yan
 640 et al., 2018). Moreover, $Lev-C$ moderately correlated with the EC_{fossil} with the regression
 641 slope (~ 0.01) in the Gosan samples (Figure 9b), being comparable to that observed for the
 642 coal combustion in China (0.044 ± 0.076) (Yan et al., 2018). It should be noted that excluding
 643 the three outliers as shown in Figure 9b (black square), $Lev-C$ showed a stronger correlation
 644 with EC_{fossil} ($R^2 = 0.74$, $p < 0.05$). Of these, two outliers in winter (KOS995: 22-29 January
 645 2014; KOS996: 21 February - 3 March 2014) have higher $Lev-C$ levels over that of EC_{fossil} ,
 646 when air mass trajectories showed the impact of BB emissions in the North China Plain. In
 647 contrast, the third outlier in summer (KOS979: 1-11 June 2013) has a lower $Lev-C/EC_{fossil}$,
 648 while air parcels transported from nearby cities in China, Korea, and Japan, thus, have more
 649 contribution from vehicular emissions. Overall, both regression slopes are, thus, the
 650 representative nature of $Lev-C/OC_{fossil}$ and $Lev-C/EC_{fossil}$ in the East Asian outflow. $Lev-C$ and
 651 $nss-SO_4^{2-}$ exhibited a poor correlation (Figure 9c), although both were transported from East
 652 Asia.

653 $Lev-C$ exhibited a rather weaker correlation with $OC_{nonfossil}$ ($R^2 = 0.19$) than with
 654 $EC_{nonfossil}$ ($R^2 = 0.42$) over Gosan during the study period (Figure 9d-e). This could be likely
 655 because $OC_{nonfossil}$ has contributions from the BB and the secondary formation process or the
 656 primary biogenic sources. The contribution of primary OC generated from BB (POC_{BB}) to
 657 $OC_{nonfossil}$ was taken from Zhang et al. (2016). In their study, the ^{14}C -based $EC_{nonfossil}$ levels
 658 were scaled by a factor to constrain the POC_{BB} (Zhang et al., 2016). Here the conversion
 659 factor is '4.5' (range: 3-10), which is a median value representing the primary OC/EC ratio
 660 from BB emissions ($(POC/EC)_{BB}$).

$$661 \quad POC_{BB} = EC_{nonfossil} \times (POC/EC)_{BB} \quad (7)$$

662 $Lev-C$ showed a somewhat improved linear correlation with POC_{BB} than with $OC_{nonfossil}$
 663 (Figure 9f). It is apparent from Figure 9 that the regression slopes are comparable, indicating
 664 the contribution to Lev from both coal combustion and BB emissions over Gosan. The
 665 prevailing weak linear relationship (moderate correlation) of Lev with nonfossil and fossil
 666 carbon fractions is likely the result of photo-degradation of Lev during atmospheric transport.
 667 This result would mean that the higher atmospheric abundance of Lev and its pronounced
 668 linear relationships with the nonfossil and fossil carbon fractions implies a much stronger
 669 impact of both source emissions in East Asia during the continental outflow in winter and
 670 spring.

671 Overall, we present a new finding on the contribution of coal combustion sources in East
672 Asia in controlling the atmospheric levels of *Lev* apart from the traditional biomass/biofuel
673 burning emissions. This is based on the prevailing linear relationship between the
674 radiocarbon based nonfossil-EC and *Lev* in the year-round TSP samples collected from the
675 KCOG site in Jeju Island. The Gosan supersite is the best location to understand how the
676 chemical composition of source emissions from East Asia affects the outflow regions in
677 winter and spring. Recent studies have highlighted the potential contribution of *Lev* from
678 residential coal combustion in China (Yan et al., 2018), with an estimated annual emission of
679 ~2.2 Gg of *Lev* from domestic coal combustion (Wu et al., 2021). Given this background
680 information, the prevailing significant linear relationship between *Lev* and nonfossil-EC (p -
681 value < 0.05) over the KCOG clearly emphasizes the need for reconsideration of the previous
682 assessments on the impact of BB in East Asian outflow to the WNP. Additionally, this
683 dataset is further compared with the molecular distributions and relative abundances of
684 organic tracers in the TSP samples collected over Gosan during 2001, a decade ago (Fu et al.,
685 2012a). This comparison allows us to better understand the regional changes in the emission
686 sources (e.g., fugitive dust, BB, and fossil-fuel combustion) on a decadal basis.

687 **4. Conclusions**

688 We investigated seasonal variations of primary organic components such as anhydrosugars,
689 primary sugars, sugar alcohols and BSOA tracers (isoprene- and monoterpene-derived SOA
690 products) in ambient aerosols from Gosan, Jeju Island. Among the detected sugar
691 compounds, levoglucosan was dominant in winter/fall, whereas glucose and sucrose were
692 more abundant in spring/summer. The seasonal trends documented that BB impact is more
693 significant in winter/fall and the primary bioaerosol particles are important in spring/summer.
694 Diagnostic ratios of levoglucosan, galactosan, and mannosan reflect that emissions from BB
695 are mostly dominated by hardwood. The significant linear relationship of sucrose with
696 glucose and fructose suggests their origin from airborne pollen. On a similar note, trehalose
697 showed a significant positive correlation with arabitol, mannitol, and erythritol, implying
698 their contribution from airborne fungal spores and soil microbes over the KCOG.

699 Distributions of biogenic SOA tracers were characterized by a predominance of
700 monoterpene- than isoprene-derived oxidation products in Gosan aerosols. The BSOA tracers
701 were formed in summer to a greater extent, followed by fall/spring and then winter. The low
702 ratio of *cis*-pinonic acid + pinic acid to MBTCA demonstrated that monoterpene-SOA was
703 relatively aged over Gosan aerosols. The estimated SOC with the predominance in summer

704 shows that substantial BSOA formation occurred in summer due to favorable meteorological
705 conditions. The backward air mass trajectories and source apportionment studies entirely
706 demonstrated that emission from East Asia significantly dominates the ambient OA mass
707 over KCOG. Interestingly, levoglucosan-C exhibited a significant positive correlation with
708 nonfossil and fossil organic carbon fractions, along with the comparable regression slopes.
709 This result reveals that BB and coal (lignite) combustion both are prominent sources for
710 levoglucosan in the East Asian outflow.

711 Although there is some evidence that levoglucosan could originate from the
712 combustion of brown coals (e.g., lignite) in China, our observations from the KCOG
713 (receptor site) also hint at the fossil source contribution of this molecular marker in the
714 regional influx of the East Asian outflow. Therefore, attribution of ambient levoglucosan
715 levels over the WNP to the impact of BB emission may cause large uncertainty.

716 **Data availability**

717 The data used in this paper are available upon request from the corresponding author.

718 **Author contributions**

719 KK and YLZ designed the research. ML collected the aerosol samples. MMH and SB
720 performed the analysis of aerosol samples. MMH wrote the paper under the guidance of YLZ
721 and KK. All authors were actively involved in the discussion of the paper.

722 **Competing interests**

723 The authors declare that they have no conflict of interest.

724 **Acknowledgments**

725 We acknowledge the financial supports of the Japan Society for the Promotion of Science
726 (JSPS) through Grant-in-Aid No. 24221001 and the National Natural Science Foundation of
727 China (Grant No 41977305).

728

729

730 **References**

- 731 Arimoto, R., Duce, R. A., Savoie, D. L., Prospero, J. M., Talbot, R., Cullen, J. D., Tomza, U.,
732 Lewis, N. F., and Ray, B. J.: Relationships among aerosol constituents from Asia and the
733 North Pacific during PEM-West A, *J. Geophys. Res. Atmos.*, 101, 2011-2023,
734 <https://doi.org/10.1029/95JD01071>, 1996.
- 735 Bauer, H., Claeys, M., Vermeylen, R., Schueller, E., Weinke, G., Berger, A., and Puxbaum,
736 H.: Arabitol and mannitol as tracers for the quantification of airborne fungal spores,
737 *Atmos. Environ.*, 42, 588–593, 2008.
- 738 Bikkina, S., Haque, M. M., Sarin, M., and Kawamura, K.: Tracing the relative significance of
739 primary versus secondary organic aerosols from biomass burning plumes over coastal

- 740 ocean using sugar compounds and stable carbon isotopes, *ACS Earth Space Chem.*, 3,
741 1471-1484, <https://doi.org/10.1021/acsearthspacechem.9b00140>, 2019.
- 742 Bikkina, S., Kawamura, K., Sakamoto, Y., and Hirokawa, J: Low molecular weight
743 dicarboxylic acids, oxocarboxylic acids and α -dicarbonyls as ozonolysis products of
744 isoprene: Implication for the gaseous-phase formation of secondary organic aerosols, *Sci.*
745 *Total Environ.*, 769, 144472, <https://doi.org/10.1016/j.scitotenv.2020.144472>, 2021.
- 746 Birch, M. E. and Cary, R. A.: Elemental carbon-based method for monitoring occupational
747 exposures to particulate diesel exhaust, *Aerosol Sci. Technol.*, 25 (3), 221–241, 1996.
- 748 Boreddy, S. K. R., Haque, M. M., and Kawamura, K.: Long term (2001–2012) trends of
749 carbonaceous aerosols from a remote island in the western North Pacific: an outflow
750 region of Asian pollutants, *Atmos. Chem. Phys.*, 18, 1291–1306,
751 <https://doi.org/10.5194/acp-18-1291-2018>, 2018.
- 752 Broadgate, W. J., Liss, P. S., and Penkett, S. A.: Seasonal emissions of isoprene and other
753 reactive hydrocarbon gases from the ocean, *Geophys. Res. Lett.*, 24, 2675-2678,
754 <https://doi.org/10.1029/97GL02736>, 1997.
- 755 Cheng, Y., Engling, G., He, K.-B., Duan, F.-K., Ma, Y.-L., Du, Z.-Y., Liu, J.-M., Zheng, M.,
756 and Weber, R. J.: Biomass burning contribution to Beijing aerosol, *Atmos. Chem. Phys.*,
757 13, 7765–7781, 2013.
- 758 Claeys, M., Graham, B., Vas, G., Wang, W., Vermeylen, R., Pashynska, V., Cafmeyer, J.,
759 Guyon, P., Andreae, M. O., Artaxo, P., and Maenhaut, W.: Formation of secondary
760 organic aerosols through photooxidation of isoprene, *Science*, 303(5661), 1173–1176,
761 2004.
- 762 Claeys, M., Szmigielski, R., Kourtshev, I., van der Veken, P., Vermeylen, R., Maenhaut, W.,
763 Jaoui, M., Kleindienst, T. E., Lewandowski, M., Offenberg, J., and Edney, E. O.:
764 Hydroxydicarboxylic acids: Markers for secondary organic aerosol from the
765 photooxidation of α -pinene, *Environ. Sci. Technol.*, 41(5), 1628–1634, 2007.
- 766 Conte, L., Szopa, S., Aumont, O., Gros, V., and Bopp, L.: Sources and sinks of isoprene in
767 the global open ocean: Simulated patterns and emissions to the atmosphere, *J. Geophys.*
768 *Res. Ocean.*, 9, e2019JC015946, <https://doi.org/10.1029/2019JC015946>, 2020.
- 769 Deguillaume, L., Leriche, M., Amato, P., Ariya, P. A., Delort, A.-M., Pöschl, U.,
770 Chaumerliac, N., Bauer, H., Flossmann, A. I., and Morris, C. E.: Microbiology and
771 atmospheric processes: chemical interactions of primary biological aerosols,
772 *Biogeosciences*, 5, 1073–1084, 2008.
- 773 Ding, X., Wang, X. M., Gao, B., Fu, X. X., He, Q. F., Zhao, X. Y., Yu, J. Z., and Zheng, M.:
774 Tracer-based estimation of secondary organic carbon in the Pearl River Delta, south
775 China, *J. Geophys. Res. Atmos.*, 117, D05313, <https://doi.org/10.1029/2011JD016596>,
776 2012.
- 777 Ding, X., He, Q. F., Shen, R. Q., Yu, Q. Q., and Wang, X. M.: Spatial distributions of
778 secondary organic aerosols from isoprene, monoterpenes, β -caryophyllene, and aromatics
779 over China during summer, *J. Geophys. Res.*, 119, 11877-11891,
780 <https://doi.org/10.1002/2014JD021748>, 2014.
- 781 Engling, G., Carrico, C. M., Kreidenweis, S. M., Collett, J. L., Day, D. E., Malm, W. C.,
782 Lincoln, E., Hao, W. M., Iinuma, Y., and Herrmann, H.: Determination of levoglucosan

- 783 in biomass combustion aerosol by high-performance anion-exchange chromatography
784 with pulsed amperometric detection, *Atmos. Environ.*, 40, S299–S311, 2006.
- 785 Engling, G., Lee, J. J., Tsai, Y. W., Lung, S. C. C., Chou, C. C. K., and Chan, C. Y.: Size-
786 resolved anhydrosugar composition in smoke aerosol from controlled field burning of rice
787 straw, *Aerosol Sci. Technol.*, 43(7), 662–672,
788 <https://doi.org/10.1080/02786820902825113>, 2009.
- 789 Fabbri, D., Marynowski, L., Fabianska, M. J., Zaton, M., and Simoneit, B. R. T.:
790 Levoglucosan and other cellulose markers in pyrolysates of miocene lignites:
791 Geochemical and environmental implications, *Environ. Sci. Technol.*, 42(8), 2957–2963,
792 <https://doi.org/10.1021/Es7021472>, 2008.
- 793 Fine, P. M., Cass, G. R., and Simoneit, B. R. T.: Chemical characterization of fine particle
794 emissions from fireplace combustion of woods grown in the northeastern United States,
795 *Environ. Sci. Technol.*, 35(13), 2665–2675, 2001.
- 796 Fine, P. M., Cass, G. R., and Simoneit, B. R. T.: Chemical characterization of fine particle
797 emissions from the fireplace combustion of wood types grown in the Midwestern and
798 Western United States, *Environ. Eng. Sci.*, 21(3), 387–409, 2004.
- 799 Fraser, M. P. and Lakshmanan, K.: Using levoglucosan as a molecular marker for the long-
800 range transport of biomass combustion aerosols, *Environ. Sci. Technol.*, 34(21), 4560–
801 4564, <https://doi.org/10.1021/es991229l>, 2000.
- 802 Fu, P., Kawamura, K., Kanaya, Y., and Wang, Z.: Contributions of biogenic volatile organic
803 compounds to the formation of secondary organic aerosols over Mt. Tai, Central East
804 China, *Atmos. Environ.*, 44, 4817–4826, <https://doi.org/10.1016/j.atmosenv.2010.08.040>,
805 2010a.
- 806 Fu, P., Kawamura, K., Kobayashi, M., and Simoneit, B. R. T.: Seasonal variations of sugars
807 in atmospheric particulate matter from Gosan, Jeju Island: Significant contributions of
808 airborne pollen and Asian dust in spring, *Atmos. Environ.*, 55, 234–239,
809 <https://doi.org/10.1016/j.atmosenv.2012.02.061>, 2012a.
- 810 Fu, P. Q., Kawamura, K., Okuzawa, K., Aggarwal, S. G., Wang, G., Kanaya, Y., and Wang,
811 Z.: Organic molecular compositions and temporal variations of summertime mountain
812 aerosols over Mt. Tai, North China Plain, *J. Geophys. Res. Atmos.*, 113, D1910,
813 <https://doi.org/10.1029/2008JD009900>, 2008.
- 814 Fu, P. Q., Kawamura, K., and Barrie, L. A.: Photochemical and other sources of organic
815 compounds in the Canadian high Arctic aerosol pollution during winter-spring, *Environ.*
816 *Sci. Technol.*, 43(2), 286–292, 2009a.
- 817 Fu, P. Q., Kawamura, K., Chen, J., and Barrie, L. A.: Isoprene, monoterpene, and
818 sesquiterpene oxidation products in the high Arctic aerosols during late winter to early
819 summer, *Environ. Sci. Technol.*, 43(11), 4022–4028, 2009b.
- 820 Fu, P. Q., Kawamura, K., Pavuluri, C. M., Swaminathan, T., and Chen, J.: Molecular
821 characterization of urban organic aerosol in tropical India: contributions of primary
822 emissions and secondary photooxidation, *Atmos. Chem. Phys.*, 10(6), 2663–2689, 2010b.
- 823 Fu, P. Q., Kawamura, K., and Miura, K.: Molecular characterization of marine organic
824 aerosols collected during a round-the-world cruise, *J. Geophys. Res.*, 116, D13302,
825 <https://doi.org/10.1029/2011jd015604>, 2011.

- 826 Fu, P. Q., Kawamura, K., Chen, J., Li, J., Sun, Y. L., Liu, Y., Tachibana, E., Aggarwal, S. G.,
827 Okuzawa, K., Tanimoto, H., Kanaya, Y., and Wang, Z. F.: Diurnal variations of organic
828 molecular tracers and stable carbon isotopic composition in atmospheric aerosols over
829 Mt. Tai in the North China Plain: an influence of biomass burning, *Atmos. Chem. Phys.*,
830 12(18), 8359–8375, <https://doi.org/10.5194/Acp-12-8359-2012>, 2012b.
- 831 Gómez-González, Y., Wang, W., Vermeylen, R., Chi, X., Neiryneck, J., Janssens, I. A.,
832 Maenhaut, W., and Claeys, M.: Chemical characterisation of atmospheric aerosols during
833 a 2007 summer field campaign at Brasschaat, Belgium: Sources and source processes of
834 biogenic secondary organic aerosol, *Atmos. Chem. Phys.*, 12, 125–138,
835 <https://doi.org/10.5194/acp-12-125-2012>, 2012.
- 836 Graham, B., Guyon, P., Taylor, P. E., Artaxo, P., Maenhaut, W., Glovsky, M. M., Flagan, R.
837 C., and Andreae, M. O.: Organic compounds present in the natural Amazonian aerosol:
838 Characterization by gas chromatography-mass spectrometry, *J. Geophys. Res. Atmos.*,
839 108, D24, 4766, <https://doi.org/10.1029/2003JD003990>, 2003.
- 840 Griffin, R. J., Cocker, D. R., Seinfeld, J. H., and Dabdub, D.: Estimate of global atmospheric
841 organic aerosol from oxidation of biogenic hydrocarbons, *Geophys. Res. Lett.*, 26, 2721–
842 2724, 1999.
- 843 Guenther, A., Hewitt, C. N., Erickson, D., Fall, R., Geron, C., Graedel, T., Harley, P.,
844 Klinger, L., Lerdau, M., McKay, W. A., Pierce, T., Scholes, B. R. S., Tallamraju, R.,
845 Taylor, J., and Zimmerman, P.: A global model of natural volatile organic compound
846 emissions, *J. Geophys. Res.*, 100(D5), 8873–8892, 1995.
- 847 Guenther, A., Karl, T., Harley, P., Wiedinmyer, C., Palmer, P. I., and Geron, C.: Estimates of
848 global terrestrial isoprene emissions using MEGAN (Model of Emissions of Gases and
849 Aerosols from Nature), *Atmos. Chem. Phys.*, 6, 3181–3210, 2006.
- 850 Haque, M. M., Kawamura, K., Deshmukh, D. K., Fang, C., Song, W., Mengying, B., and
851 Zhang, Y. L.: Characterization of organic aerosols from a Chinese megacity during
852 winter: Predominance of fossil fuel combustion, *Atmos. Chem. Phys.*, 19, 5147–5164,
853 <https://doi.org/10.5194/acp-19-5147-2019>, 2019.
- 854 Heald, C. L. and Spracklen, D. V.: Atmospheric budget of primary biological aerosol
855 particles from fungal spores, *Geophys. Res. Lett.*, 36, L09806,
856 <https://doi.org/10.1029/2009GL037493>, 2009.
- 857 Heald, C. L., Henze, D. K., Horowitz, L. W., Feddema, J., Lamarque, J. F., Guenther, A.,
858 Hess, P. G., Vitt, F., Seinfeld, J. H., Goldstein, A. H., and Fung, I.: Predicted change in
859 global secondary organic aerosol concentrations in response to future climate, emissions,
860 and land use change, *J. Geophys. Res.*, 113(D5), <https://doi.org/10.1029/2007jd009092>,
861 2008.
- 862 Hennigan, C. J., Sullivan, A. P., Collett, J. L., and Robinson, A. L.: Levoglucosan stability in
863 biomass burning particles exposed to hydroxyl radicals, *Geophys. Res. Lett.*, 37,
864 <https://doi.org/10.1029/2010GL043088>, 2010.
- 865 Hu, Q. H., Xie, Z. Q., Wang, X. M., Kang, H., He, Q. F., and Zhang, P.: Secondary organic
866 aerosols over oceans via oxidation of isoprene and monoterpenes from Arctic to
867 Antarctic, *Sci. Rep.*, 3, 3119, <https://doi.org/10.1038/srep02280>, 2013.
- 868 Huang, R. J., Zhang, Y-L., Bozzetti, C., Ho, K-F., Cao, J-J., Han, Y., Daellenbach, K. R.,
869 Slowik, J. G., Platt, S. M., Canonaco, F., Zotter, P., Wolf, R., Pieber, S. M., Bruns, E. A.,

- 870 Crippa, M., Ciarelli, G., Piazzalunga, A., Schwikowski, M., Abbaszade, G., Schnelle-
871 Kreis, J., Zimmermann, R., An, Z., Szidat, S., Baltensperger, U., Haddad, I. E., and Pr  t,
872 A. S. H.: High secondary aerosol contribution to particulate pollution during haze events
873 in China, *Nature*, 514, 218–222, <https://doi.org/10.1038/nature13774>, 2014.
- 874 Huebert, B. J., Bates, T., Russell, P. B., Shi, G. Y., Kim, Y. J., Kawamura, K., Carmichael,
875 G., and Nakajima, T.: An overview of ACE-Asia: Strategies for quantifying the
876 relationships between Asian aerosols and their climatic impacts, *J. Geophys. Res. Atmos.*,
877 108(D23), 8633, <https://doi.org/10.1029/2003JD003550>, 2003.
- 878 Jia, Y. L. and Fraser, M.: Characterization of saccharides in size-fractionated ambient
879 particulate matter and aerosol sources: The contribution of primary biological aerosol
880 particles (PBAPs) and soil to ambient particulate matter, *Environ. Sci. Technol.*, 45(3),
881 930–936, <https://doi.org/10.1021/es103104e>, 2011.
- 882 Kanakidou, M., Seinfeld, J. H., Pandis, S. N., Barnes, I., Dentener, F. J., Facchini, M. C., Van
883 Dingenen, R., Ervens, B., Nenes, A., Nielsen, C. J., Swietlicki, E., Putaud, J. P.,
884 Balkanski, Y., Fuzzi, S., Horth, J., Moortgat, G. K., Winterhalter, R., Myhre, C. E. L.,
885 Tsigaridis, K., Vignati, E., Stephanou, E. G., and Wilson, J.: Organic aerosol and global
886 climate modelling: a review, *Atmos. Chem. Phys.*, 5, 1053–1123, 2005.
- 887 Kang, M., Ren, L., Ren, H., Zhao, Y., Kawamura, K., Zhang, H., Wei, L., Sun, Y., Wang, Z.,
888 and Fu, P.: Primary biogenic and anthropogenic sources of organic aerosols in Beijing,
889 China: Insights from saccharides and n-alkanes, *Environ. Pollut.*, 243, 1579–1587,
890 <https://doi.org/10.1016/j.envpol.2018.09.118>, 2018a.
- 891 Kang, M., Fu, P., Kawamura, K., Yang, F., Zhang, H., Zang, Z., Ren, H., Ren, L., Zhao, Y.,
892 Sun, Y., and Wang, Z.: Characterization of biogenic primary and secondary organic
893 aerosols in the marine atmosphere over the East China Sea, *Atmos. Chem. Phys.*, 19,
894 13947–13967, <https://doi.org/10.5194/acp-18-13947-2018>, 2018b.
- 895 Kawamura, K., Kobayashi, M., Tsubonuma, N., Mochida, M., Watanabe, T., and Lee, M.:
896 Organic and inorganic compositions of marine aerosols from East Asia: Seasonal
897 variations of water-soluble dicarboxylic acids, major ions, total carbon and nitrogen, and
898 stable C and N isotopic composition, in *geochemical investigations in earth and space
899 science: A Tribute to Isaac R. Kaplan*, edited by R. J. Hill, J. Leventhal, Z. Aizenshtat, M.
900 J. Baedeker, G. Claypool, R. Eganhouse, M. Goldhaber, and K. Peters, pp. 243–265, The
901 Geochemical Society, 2004.
- 902 Kessler, S. H., Smith, J. D., Che, D. L., Worsnop, D. R., Wilson, K. R., and Kroll, J. H.:
903 Chemical sinks of organic aerosol: Kinetics and products of the heterogeneous oxidation
904 of erythritol and levoglucosan, *Environ. Sci. Technol.*, 44(18), 7005–7010,
905 <https://doi.org/10.1021/Es101465m>, 2010.
- 906 Kleindienst, T. E., Jaoui, M., Lewandowski, M., Offenberg, J. H., Lewis, C. W., Bhave, P.
907 V., and Edney, E. O.: Estimates of the contributions of biogenic and anthropogenic
908 hydrocarbons to secondary organic aerosol at a southeastern US location, *Atmos.*
909 *Environ.*, 41, 8288–8300, 2007.
- 910 Kourtchev, I., Hellebust, S., Bell, J. M., O’Connor, I. P., Healy, R. M., Allanic, A., Healy, D.,
911 Wenger, J. C., and Sodeau, J. R.: The use of polar organic compounds to estimate the
912 contribution of domestic solid fuel combustion and biogenic sources to ambient levels of

- 913 organic carbon and PM_{2.5} in Cork Harbour, Ireland, *Sci. Total Environ.*, 11, 2143-2155,
914 <https://doi.org/10.1016/j.scitotenv.2011.02.027>, 2011.
- 915 Kroll, J. H., Ng, N. L., Murphy, S. M., Flagan, R. C., and Seinfeld, J. H.: Secondary organic
916 aerosol formation from isoprene photooxidation under high-NO_x conditions, *Geophys.*
917 *Res. Lett.*, 32(18), L18808, <https://doi.org/10.1029/2005gl023637>, 2005.
- 918 Kroll, J. H., Ng, N. L., Murphy, S. M., Flagan, R. C., and Seinfeld, J. H.: Secondary organic
919 aerosol formation from isoprene photooxidation, *Environ. Sci. Technol.*, 40, 1869–1877,
920 2006.
- 921 Kundu, S., Kawamura, K., and Lee, M.: Seasonal variations of diacids, ketoacids, and α -
922 dicarbonyls in aerosols at Gosan, Jeju Island, South Korea: Implications for sources,
923 formation, and degradation during long-range transport, *J. Geophys. Res.*, 115, D19307,
924 <https://doi.org/10.1029/2010jd013973>, 2010.
- 925 Liu, J., Chu, B., Chen, T., Liu, C., Wang, L., Bao, X., and He, H.: Secondary organic aerosol
926 formation from ambient air at an urban site in Beijing: Effects of OH exposure and
927 precursor concentrations, *Environ. Sci. Technol.*, 52, 6834-6841,
928 <https://doi.org/10.1021/acs.est.7b05701>, 2018.
- 929 Medeiros, P. M. and Simoneit, B. R. T.: Analysis of sugars in environmental samples by gas
930 chromatography-mass spectrometry, *J. Chromatogr. A*, 1141(2), 271–278,
931 <https://doi.org/10.1016/j.chroma.2006.12.017>, 2007.
- 932 Medeiros, P. M., Conte, M. H., Weber, J. C., and Simoneit, B. R. T.: Sugars as source
933 indicators of biogenic organic carbon in aerosols collected above the Howland
934 Experimental Forest, Maine, *Atmos. Environ.*, 40(9), 1694–1705, 2006.
- 935 Mohn, J., Szidat, S., Fellner, J., Rechberger, H., Quartier, R., Buchmann, B., and
936 Emmenegger, L.: Determination of biogenic and fossil CO₂ emitted by waste incineration
937 based on ¹⁴CO₂ and mass balances, *Bioresour. Technol.*, 99, 6471-6479,
938 <https://doi.org/10.1016/j.biortech.2007.11.042>, 2008.
- 939 Müller, L., Reining, M. C., Naumann, K. H., Saathoff, H., Mentel, T. F., Donahue, N. M.,
940 and Hoffmann, T.: Formation of 3-methyl-1,2,3-butanetricarboxylic acid via gas phase
941 oxidation of pinonic acid - A mass spectrometric study of SOA aging, *Atmos. Chem.*
942 *Phys.*, 12, 1483-1496, <https://doi.org/10.5194/acp-12-1483-2012>, 2012.
- 943 Nakajima, T., Yoon, S. C., Ramanathan, V., Shi, G. Y., Takemura, T., Higurashi, A.,
944 Takamura, T., Aoki, K., Sohn, B. J., Kim, S. W., Tsuruta, H., Sugimoto, N., Shimizu, A.,
945 Tanimoto, H., Sawa, Y., Lin, N. H., Lee, C. T., Goto, D., and Schutgens, N.: Overview of
946 the atmospheric brown cloud east Asian regional experiment 2005 and a study of the
947 aerosol direct radiative forcing in east Asia, *J. Geophys. Res. Atmos.*, 112, D24S91,
948 <https://doi.org/10.1029/2007JD009009>, 2007.
- 949 Ng, N. L., Kwan, A. J., Surratt, J. D., Chan, A. W. H., Chhabra, P. S., Sorooshian, A., Pye, H.
950 O. T., Crounse, J. D., Wennberg, P. O., Flagan, R. C., and Seinfeld, J. H.: Secondary
951 organic aerosol (SOA) formation from reaction of isoprene with nitrate radicals (NO₃),
952 *Atmos. Chem. Phys.*, 8(14), 4117–4140, 2008.
- 953 Offenberg, J., Lewis, C., Lewandowski, M., Jaoui, M., Kleindienst, T. E., and Edney, E. O.:
954 Contributions of toluene and α -pinene to SOA formed in an irradiated toluene/ α -
955 pinene/NO_x/air mixture: Comparison of results using ¹⁴C content and SOA organic tracer
956 methods, *Environ. Sci. Technol.*, 41, 3972–3976, 2007.

- 957 Pashynska, V., Vermeylen, R., Vas, G., Maenhaut, W., and Claeys, M.: Development of a gas
958 chromatographic/ion trap mass spectrometric method for the determination of
959 levoglucosan and saccharidic compounds in atmospheric aerosols. Application to urban
960 aerosols, *J. Mass Spectrom.*, 37(12), 1249–1257, 2002.
- 961 Pio, C., Legrand, M., Alves, C. A., Oliveira, T., Afonso, J., Caseiro, A., Puxbaum, H.,
962 Sánchez-Ochoa, A., and Gelencsér, A.: Chemical composition of atmospheric aerosols
963 during the 2003 summer intense forest fire period, *Atmos. Environ.*, 42, 7530–7543,
964 2008.
- 965 Ramanathan, V., Li, F., Ramana, M. V., Praveen, P. S., Kim, D., Corrigan, C. E., Nguyen, H.,
966 Stone, E. A., Schauer, J. J., Carmichael, G. R., Adhikary, B., and Yoon, S. C.:
967 Atmospheric brown clouds: Hemispherical and regional variations in long-range
968 transport, absorption, and radiative forcing, *J. Geophys. Res. Atmos.*, 112, D22S21,
969 <https://doi.org/10.1029/2006JD008124>, 2007.
- 970 Robinson, A. L., Donahue, N. M., Shrivastava, M. K., Weitkamp, E. A., Sage, A. M.,
971 Grieshop, A. P., Lane, T. E., Pierce, J. R., and Pandis, S. N.: Rethinking organic aerosols:
972 Semivolatile emissions and photochemical aging, *Science*, 315, 1259–1262, 2007.
- 973 Salazar, G., Zhang, Y. L., Agrios, K., and Szidat, S.: Development of a method for fast and
974 automatic radiocarbon measurement of aerosol samples by online coupling of an
975 elemental analyzer with a MICADAS AMS, *Nucl. Instruments Methods Phys. Res. Sect.*
976 *B Beam Interact. with Mater. Atoms*, 361, 163–167,
977 <https://doi.org/10.1016/j.nimb.2015.03.051>, 2015.
- 978 Schmidl, C., Marr, I. L., Caseiro, A., Kotianova, P., Berner, A., Bauer, H., Kasper-Giebl, A.,
979 and Puxbaum, H.: Chemical characterisation of fine particle emissions from wood stove
980 combustion of common woods growing in mid-European Alpine regions, *Atmos.*
981 *Environ.*, 42, 126–141, 2008a.
- 982 Schmidl, C., Bauer, H., Dattler, A., Hitzenberger, R., Weissenboeck, G., Marr, I. L., and
983 Puxbaum, H.: Chemical characterisation of particle emissions from burning leaves,
984 *Atmos. Environ.*, 42(40), 9070–9079, <https://doi.org/10.1016/J.Atmosenv.2008.09.010>,
985 2008b.
- 986 Shaw, S. L., Gantt, B., and Meskhidze, N.: Production and emissions of marine isoprene and
987 monoterpenes: A Review, *Adv. Meteorol.*, 2010, 408696,
988 <https://doi.org/10.1155/2010/408696>, 2010.
- 989 Sheesley, R. J., Schauer, J. J., Chowdhury, Z., Cass, G. R., and Simoneit, B. R. T.:
990 Characterization of organic aerosols emitted from the combustion of biomass indigenous
991 to South Asia, *J. Geophys. Res.*, 108 (D9), 4285, <https://doi.org/10.1029/2002JD002981>,
992 2003.
- 993 Simoneit, B. R. T.: Biomass burning—a review of organic tracers for smoke from incomplete
994 combustion, *Appl. Geochem.*, 17, 129–162, 2002.
- 995 Simoneit, B. R. T., Schauer, J. J., Nolte, C. G., Oros, D. R., Elias, V. O., Fraser, M. P.,
996 Rogge, W. F., and Cass, G. R.: Levoglucosan, a tracer for cellulose in biomass burning
997 and atmospheric particles, *Atmos. Environ.*, 33(2), 173–182,
998 [https://doi.org/10.1016/S1352-2310\(98\)00145-9](https://doi.org/10.1016/S1352-2310(98)00145-9), 1999.
- 999 Simoneit, B. R. T., Elias, V. O., Kobayashi, M., Kawamura, K., Rushdi, A. I., Medeiros, P.
1000 M., Rogge, W. F., and Didyk, B. M.: Sugars-dominant water-soluble organic compounds

- 1001 in soils and characterization as tracers in atmospheric particulate matter, *Environ. Sci.*
1002 *Technol.*, 38(22), 5939–5949, 2004a.
- 1003 Simoneit, B. R. T., Kobayashi, M., Mochida, M., Kawamura, K., Lee, M., Lim, H-J., Turpin,
1004 B. J., and Komazaki, Y.: Composition and major sources of organic compounds of
1005 aerosol particulate matter sampled during the ACE-Asia campaign, *J. Geophys. Res.*,
1006 109(D19), D19S10, <https://doi.org/10.1029/2004jd004598>, 2004b.
- 1007 Singh, N., Mhawish, A., Deboudt, K., Singh, R. S., and Banerjee, T.: Organic aerosols over
1008 Indo-Gangetic Plain: Sources, distributions and climatic implications, *Atmos. Environ.*,
1009 157, 59-74, <https://doi.org/10.1016/j.atmosenv.2017.03.008>, 2017.
- 1010 Stein, A. F., Draxler, R. R., Rolph, G. D., Stunder, B. J. B., Cohen, M. D., and Ngan, F.:
1011 NOAA's HYSPLIT atmospheric transport and dispersion modeling system, *Bull. Am.*
1012 *Meteorol. Soc.*, 96, 2059-2077, <https://doi.org/10.1175/BAMS-D-14-00110.1>, 2015.
- 1013 Stuiver, M. and Polach, H. A.: Discussion: Reporting of ^{14}C data, *Radiocarbon*, 19(3),
1014 355–363, 1997.
- 1015 Sullivan, A. P., Holden, A. S., Patterson, L. A., McMeeking, G. R., Kreidenweis, S. M.,
1016 Malm, W. C., Hao, W. M., Wold, C. E., and Collett, Jr., J. L.: A method for smoke
1017 marker measurements and its potential application for determining the contribution of
1018 biomass burning from wildfires and prescribed fires to ambient $\text{PM}_{2.5}$ organic carbon, *J.*
1019 *Geophys. Res.*, 113, D22302, <https://doi.org/10.1029/2008JD010216>, 2008.
- 1020 Surratt, J. D., Murphy, S. M., Kroll, J. H., Ng, N. L., Hildebrandt, L., Sorooshian, A.,
1021 Szmigielski, R., Vermeylen, R., Maenhaut, W., Claeys, M., Flagan, R. C., and Seinfeld, J.
1022 H.: Chemical composition of secondary organic aerosol formed from the photooxidation
1023 of isoprene, *J. Phys. Chem. A*, 110(31), 9665–9690, 2006.
- 1024 Surratt, J. D., Chan, A. W. H., Eddingsaas, N. C., Chan, M. N., Loza, C. L., Kwan, A. J.,
1025 Hersey, S. P., Flagan, R. C., Wennberg, P. O., and Seinfeld, J. H.: Reactive intermediates
1026 revealed in secondary organic aerosol formation from isoprene, *Proc. Natl. Acad. Sci.*
1027 *USA*, 107(15), 6640–6645, 2010.
- 1028 Szidat, S., Jenk, T. M., Synal, H. A., Kalberer, M., Wacker, L., Hajdas, I., Kasper-Giebl, A.,
1029 and Baltensperger, U.: Contributions of fossil fuel, biomass-burning, and biogenic
1030 emissions to carbonaceous aerosols in Zurich as traced by ^{14}C , *J. Geophys. Res. Atmos.*,
1031 111, D07206, <https://doi.org/10.1029/2005JD006590>, 2006.
- 1032 Szmigielski, R., Surratt, J. D., Gómez-González, G., Van der Veken, P., Kourtchev, I.,
1033 Vermeylen, R., Blockhuys, F., Jaoui, M., Kleindienst, T. E., Lewandowski, M.,
1034 Offenberg, J. H., Edney, E. O., Seinfeld, J. H., Maenhaut, W., and Claeys, M.: 3-Methyl-
1035 1,2,3-butanetricarboxylic acid: An atmospheric tracer for terpene secondary organic
1036 aerosol, *Geophys. Res. Lett.*, 34, L24811, <https://doi.org/10.1029/2007GL031338>, 2007.
- 1037 Theodosi, C., Panagiotopoulos, C., Nouara, A., Zarmas, P., Nicolaou, P., Violaki, K.,
1038 Kanakidou, M., Sempéré, R., and Mihalopoulos, N.: Sugars in atmospheric aerosols over
1039 the Eastern Mediterranean, *Prog. Oceanogr.*, 163, Special Issue: SI, 70-81,
1040 <https://doi.org/10.1016/j.pocean.2017.09.001>, 2018.
- 1041 Tyagi, P., Kawamura, K., Kariya, T., Bikkina, S., Fu, P., and Lee, M.: Tracing atmospheric
1042 transport of soil microorganisms and higher plant waxes in the East Asian outflow to the
1043 North Pacific Rim by using hydroxy fatty acids: Year-round observations at Gosan, Jeju
1044 Island, *J. Geophys. Res.*, 122, 4112-4131, <https://doi.org/10.1002/2016JD025496>, 2017.

- 1045 Verma, S. K., Kawamura, K., Chen, J., Fu, P., and Zhu, C.: Thirteen years of observations on
1046 biomass burning organic tracers over Chichijima Island in the western North Pacific: An
1047 outflow region of Asian aerosols, *J. Geophys. Res.*, 120, 4155-4168,
1048 <https://doi.org/10.1002/2014JD022224>, 2015.
- 1049 Verma, S. K., Kawamura, K., Chen, J., and Fu, P.: Thirteen years of observations on primary
1050 sugars and sugar alcohols over remote Chichijima Island in the western North Pacific,
1051 *Atmos. Chem. Phys.*, 18, 81-101, <https://doi.org/10.5194/acp-18-81-2018>, 2018.
- 1052 Wang, G. and Kawamura, K.: Molecular characteristics of urban organic aerosols from
1053 Nanjing: A case study of a mega-city in China, *Environ. Sci. Technol.*, 39(19), 7430–
1054 7438, 2005.
- 1055 Wang, G. H., Kawamura, K., and Lee, M.: Comparison of organic compositions in dust storm
1056 and normal aerosol samples collected at Gosan, Jeju Island, during spring 2005, *Atmos.*
1057 *Environ.*, 43(2), 219–227, <https://doi.org/10.1016/J.Atmosenv.2008.09.046>, 2009a.
- 1058 Wang, G. H., Li, J. J., Cheng, C. L., Zhou, B. H., Xie, M. J., Hu, S. Y., Meng, J. J., Sun, T.,
1059 Ren, Y. Q., Cao, J. J., Liu, S. X., Zhang, T., and Zhao, Z. Z.: Observation of atmospheric
1060 aerosols at Mt. Hua and Mt. Tai in central and east China during spring 2009-Part 2:
1061 Impact of dust storm on organic aerosol composition and size distribution, *Atmos. Chem.*
1062 *Phys.*, 12(9), 4065–4080, 2012.
- 1063 Wang, W., Kourtchev, I., Graham, B., Cafmeyer, J., Maenhaut, W., and Claeys, M.:
1064 Characterization of oxygenated derivatives of isoprene related to 2-methyltetrols in
1065 Amazonian aerosols using trimethylsilylation and gas chromatography/ion trap mass
1066 spectrometry, *Rapid Commun. Mass Spectrom.*, 19, 1343–1351, 2005.
- 1067 Wang, Y. Q., Zhang, X. Y., and Draxler, R. R.: TrajStat: GIS-based software that uses
1068 various trajectory statistical analysis methods to identify potential sources from long-term
1069 air pollution measurement data, *Environ. Model. Softw.*, 24, 938-939,
1070 <https://doi.org/10.1016/j.envsoft.2009.01.004>, 2009b.
- 1071 Wu, J., Kong, S., Zeng, X., Cheng, Y., Yan, Q., Zheng, H., Yan, Y., Zheng, S., Liu, D.,
1072 Zhang, X., Fu, P., Wang, S., and Qi, S.: First high-resolution emission inventory of
1073 levoglucosan for biomass burning and non-biomass burning sources in China, *Environ.*
1074 *Sci. Technol.*, 55, 3, 1497–1507, 2021.
- 1075 Yan, C., Zheng, M., Sullivan, A. P., Shen, G., Chen, Y., Wang, S., Zhao, B., Cai, S.,
1076 Desyaterik, Y., Li, X., Zhou, T., Gustafsson, Ö., and Collett, J. L.: Residential coal
1077 combustion as a source of levoglucosan in China, *Environ. Sci. Technol.*, 52, 3, 1665–
1078 1674, <https://doi.org/10.1021/acs.est.7b05858>, 2018.
- 1079 Yttri, K. E., Dye, C., and Kiss, G.: Ambient aerosol concentrations of sugars and sugar-
1080 alcohols at four different sites in Norway, *Atmos. Chem. Phys.*, 7, 4267–4279, 2007.
- 1081 Zangrando, R., Barbaro, E., Kirchgeorg, T., Vecchiato, M., Scalabrin, E., Radaelli, M.,
1082 Đorđević, D., Barbante, C., and Gambaro, A.: Five primary sources of organic aerosols in
1083 the urban atmosphere of Belgrade (Serbia), *Sci. Total Environ.*, 571, 1441-1453,
1084 <https://doi.org/10.1016/j.scitotenv.2016.06.188>, 2016.
- 1085 Zhang, Y. L., Perron, N., Ciobanu, V. G., Zotter, P., Minguillón, M. C., Wacker, L., Prévôt,
1086 A. S. H., Baltensperger, U., and Szidat, S.: On the isolation of OC and EC and the optimal
1087 strategy of radiocarbon-based source apportionment of carbonaceous aerosols, *Atmos.*
1088 *Chem. Phys.*, 12, 10841-10856, <https://doi.org/10.5194/acp-12-10841-2012>, 2012.

- 1089 Zhang, Y. L., Huang, R. J., El Haddad, I., Ho, K. F., Cao, J. J., Han, Y., Zotter, P., Bozzetti,
1090 C., Daellenbach, K. R., Canonaco, F., Slowik, J. G., Salazar, G., Schwikowski, M.,
1091 Schnelle-Kreis, J., Abbaszade, G., Zimmermann, R., Baltensperger, U., Prévôt, A. S. H.,
1092 and Szidat, S.: Fossil vs. non-fossil sources of fine carbonaceous aerosols in four Chinese
1093 cities during the extreme winter haze episode of 2013, *Atmos. Chem. Phys.*, 15(3), 1299-
1094 1312, <https://doi.org/10.5194/acp-15-1299-2015>, 2015.
- 1095 Zhang, Y. L., Kawamura, K., Agrios, K., Lee, M., Salazar, G., and Szidat, S.: Fossil and
1096 nonfossil sources of organic and elemental carbon aerosols in the outflow from Northeast
1097 China, *Environ. Sci. Technol.*, 50, 6284-6292, <https://doi.org/10.1021/acs.est.6b00351>,
1098 2016.
- 1099 Zhu, C., Kawamura, K., and Kunwar, B.: Effect of biomass burning over the western North
1100 Pacific Rim: wintertime maxima of anhydrosugars in ambient aerosols from Okinawa.,
1101 *Atmos. Chem. Phys.*, 15, 1959–1973, <https://doi.org/10.5194/acp-15-1959-2015>, 2015a.
- 1102 Zhu, C., Kawamura, K., and Kunwar, B.: Organic tracers of primary biological aerosol
1103 particles at subtropical Okinawa island in the western North pacific rim, *J. Geophys. Res.*,
1104 120, 5504-5523, <https://doi.org/10.1002/2015JD023611>, 2015b.
- 1105
- 1106
- 1107
- 1108
- 1109
- 1110
- 1111
- 1112
- 1113
- 1114
- 1115
- 1116
- 1117
- 1118
- 1119
- 1120

1121 **Table 1.** Concentrations of identified sugar compounds and BSOA tracers (ng m⁻³) in the atmospheric
 1122 aerosol samples from Gosan.

Species	Annual	Summer	Fall	Winter	Spring
	Avg. ^a ± S.D. ^b Min. ^c , Max. ^d	Avg. ± S.D. Min., Max.	Avg. ± S.D. Min., Max.	Avg. ± S.D. Min., Max.	Avg. ± S.D. Min., Max.
Anhydrosugars					
Levoglucozan (Lev)	17.6 ± 16.8 0.60, 45.9	2.92 ± 3.89 0.60, 9.81	21.7 ± 19.0 2.30, 43.9	39.2 ± 6.60 32.0, 45.9	12.7 ± 11.6 1.45, 33.4
Mannosan (Man)	1.57 ± 1.82 0.05, 6.74	0.18 ± 0.24 0.05, 0.61	1.69 ± 1.49 0.13, 3.66	3.63 ± 2.28 1.47, 6.74	1.31 ± 1.57 0.08, 4.08
Galactosan (Gal)	2.28 ± 2.10 0.14, 6.78	0.64 ± 0.68 0.14, 1.82	2.45 ± 2.13 0.35, 4.92	5.21 ± 1.64 3.40, 6.78	1.65 ± 1.26 0.50, 3.88
Primary Sugars					
Glucose	18.8 ± 27.1 2.45, 122	13.4 ± 18.2 2.45, 45.6	16.5 ± 15.7 2.68, 33.6	4.74 ± 3.14 2.88, 9.44	32.4 ± 41.1 4.87, 122
Fructose	10.3 ± 15.9 0.97, 74.0	4.90 ± 5.15 0.97, 13.7	7.48 ± 6.99 1.71, 16.2	3.82 ± 4.45 1.56, 10.5	19.8 ± 25.0 2.69, 74.0
Sucrose	16.1 ± 32.2 0.26, 140	1.46 ± 1.05 0.68, 3.28	9.74 ± 12.1 0.76, 27.2	8.87 ± 16.3 0.42, 33.3	35.1 ± 50.5 0.26, 140
Trehalose	2.42 ± 1.97 0.65, 7.03	2.72 ± 2.53 0.97, 6.98	3.71 ± 2.29 1.18, 7.03	1.21 ± 0.42 0.72, 1.63	1.98 ± 1.55 0.65, 5.33
Xylose	0.81 ± 0.65 0.04, 2.03	0.23 ± 0.23 0.04, 0.63	0.86 ± 0.68 0.14, 1.70	1.59 ± 0.37 1.21, 2.03	0.74 ± 0.55 0.16, 1.68
Sugar alcohols					
Arabitol	3.96 ± 4.24 0.47, 18.7	5.64 ± 7.46 1.20, 18.7	5.27 ± 3.51 2.27, 10.9	1.06 ± 0.60 0.47, 1.91	3.47 ± 2.19 1.18, 6.30
Mannitol	4.61 ± 5.54 0.25, 22.0	7.39 ± 8.65 1.71, 22.0	6.64 ± 6.03 1.69, 16.7	0.99 ± 0.45 0.55, 1.60	3.24 ± 2.67 0.25, 7.03
Erythritol	0.62 ± 0.43 0.12, 1.52	0.92 ± 0.53 0.42, 1.52	0.93 ± 0.33 0.55, 1.27	0.42 ± 0.27 0.16, 0.80	0.30 ± 0.12 0.12, 0.48
Inositol	0.34 ± 0.39 0.04, 1.53	0.29 ± 0.41 0.08, 1.03	0.56 ± 0.60 0.10, 1.53	0.13 ± 0.07 0.08, 0.23	0.35 ± 0.28 0.04, 0.73
Isoprene-SOA tracers					
2-MGA	0.99 ± 0.70 0.17, 2.79	1.61 ± 1.17 0.17, 2.79	0.95 ± 0.43 0.51, 1.61	0.67 ± 0.14 0.49, 0.81	0.76 ± 0.35 0.20, 1.32
Σ2-MLTs	1.04 ± 1.40 0.05, 5.81	2.48 ± 1.98 0.51, 5.81	1.34 ± 1.16 0.33, 2.74	0.20 ± 0.05 0.15, 0.26	0.29 ± 0.25 0.05, 0.82
ΣC5-alkene triols	0.20 ± 0.25 0.02, 1.17	0.46 ± 0.44 0.02, 1.17	0.13 ± 0.05 0.05, 0.18	0.09 ± 0.03 0.05, 0.13	0.14 ± 0.11 0.02, 0.30
Monoterpene-SOA tracers					
<i>cis</i> -pinonic acid	0.15 ± 0.14 0.02, 0.52	0.12 ± 0.13 0.03, 0.36	0.08 ± 0.06 0.02, 0.16	0.07 ± 0.03 0.02, 0.10	0.26 ± 0.17 0.08, 0.52
pinic acid	1.67 ± 1.01 0.72, 4.81	2.40 ± 1.67 0.99, 4.81	1.53 ± 0.57 0.75, 2.11	1.07 ± 0.25 0.84, 1.42	1.61 ± 0.78 0.72, 2.94
3-HGA	2.30 ± 2.38 0.19, 10.6	3.46 ± 4.39 0.19, 10.6	1.52 ± 0.77 0.76, 2.79	1.40 ± 0.39 0.94, 1.88	2.54 ± 1.83 0.38, 4.57
MBTCA	5.11 ± 4.54 0.29, 19.6	8.44 ± 6.88 3.00, 19.6	6.24 ± 3.64 1.17, 9.49	1.90 ± 0.85 0.97, 2.83	3.77 ± 2.96 0.29, 8.08

^aAverage, ^bStandard deviation, ^cMinimum, ^dMaximum. 2-MGA: 2-methylglyceric acid, 2-MLTs: 2-methyltetrols, 3-HGA: 3-hydroxyglutaric acid, MBTCA: 3-methyl-1,2,3-butanetricarboxylic acid.

1124 **Table 2.** Statistical summary of diagnostic ratios and carbonaceous components contribution in Gosan
 1125 aerosols.
 1126

Species	Annual	Summer	Fall	Winter	Spring
	Avg. ^a ± S.D. ^b Min. ^c , Max. ^d	Avg. ± S.D. Min., Max.	Avg. ± S.D. Min., Max.	Avg. ± S.D. Min., Max.	Avg. ± S.D. Min., Max.
Diagnostic ratios					
Lev/Man	15.1 ± 6.76 6.81, 31.3	17.1 ± 8.21 8.58, 28.4	13.7 ± 2.51 11.1, 17.3	13.5 ± 6.24 6.81, 21.7	15.4 ± 8.76 6.98, 31.3
Man/Gal	0.55 ± 0.32 0.10, 1.07	0.28 ± 0.13 0.10, 0.42	0.64 ± 0.20 0.37, 0.90	0.66 ± 0.27 0.43, 1.05	0.61 ± 0.43 0.16, 1.07
Lev/(Man + Gal)	4.27 ± 1.23 2.18, 6.56	3.12 ± 0.78 2.18, 4.03	5.08 ± 0.32 4.71, 5.51	4.85 ± 1.35 3.49, 6.56	4.17 ± 1.33 2.50, 6.45
Lev/K ⁺ × 10 ⁻²	5.73 ± 5.65 0.65, 23.2	1.00 ± 0.52 0.65, 1.91	3.94 ± 2.51 1.26, 6.30	12.3 ± 7.87 6.42, 23.2	6.65 ± 4.48 1.77, 15.3
Lev/OC × 10 ⁻²	0.73 ± 0.66 0.08, 2.29	0.14 ± 0.10 0.08, 0.31	0.84 ± 0.61 0.12, 1.56	1.60 ± 0.67 0.99, 2.29	0.56 ± 0.40 0.11, 1.05
Lev/WSOC × 10 ⁻²	1.09 ± 0.97 0.10, 3.46	0.20 ± 0.13 0.10, 0.42	1.25 ± 0.94 0.23, 2.21	2.33 ± 0.90 1.48, 3.46	0.92 ± 0.65 0.13, 1.69
2-MGA/2-MLTs	2.18 ± 1.59 0.33, 5.40	0.67 ± 0.43 0.33, 1.33	1.04 ± 0.49 0.41, 1.55	3.60 ± 1.43 1.90, 5.40	3.27 ± 1.17 1.60, 4.75
^e P/MBTCA	0.62 ± 0.61 0.17, 5.90	3.22 ± 0.62 2.47, 3.89	3.62 ± 1.67 1.52, 5.90	1.68 ± 0.64 0.83, 2.38	1.73 ± 1.07 0.34, 3.32
Carbonaceous components					
Isoprene derived SOC (µgC m ⁻³)	23.7 ± 23.9 2.26, 97.4	51.0 ± 32.4 8.08, 97.4	25.9 ± 17.9 8.54, 45.7	8.52 ± 1.07 7.46, 9.87	11.3 ± 6.80 2.26, 24.9
Isoprene SOC to OC (%)	1.45 ± 1.74 0.21, 6.40	3.56 ± 2.18 1.03, 6.40	1.46 ± 1.38 0.35, 3.48	0.35 ± 0.17 0.21, 0.57	0.57 ± 0.38 0.24, 1.35
Isoprene SOC to total SOC (%)	35.5 ± 15.5 13.5, 71.1	46.6 ± 20.3 26.0, 71.1	38.1 ± 10.4 21.1, 47.3	31.6 ± 7.05 24.0, 39.7	27.9 ± 15.5 13.5, 54.0
Monoterpene SOC (µgC m ⁻³)	40.1 ± 33.3 7.18, 154	62.7 ± 56.5 19.2, 154	40.7 ± 20.0 11.8, 57.7	19.3 ± 5.61 14.0, 25.2	35.5 ± 23.5 7.18, 62.7
Monoterpene SOC to OC (%)	2.0 ± 1.47 0.37, 5.74	3.65 ± 1.58 2.44, 5.74	2.15 ± 1.45 0.48, 3.88	0.87 ± 0.58 0.37, 1.48	1.58 ± 0.84 0.54, 3.13
Monoterpene SOC to total SOC (%)	64.5 ± 15.5 28.9, 86.5	53.4 ± 20.3 28.9, 74.0	61.9 ± 10.4 52.7, 78.9	68.4 ± 7.05 60.3, 76.1	72.1 ± 15.5 46.0, 86.5

^eP: *cis*-pinonic acid + pinic acid

Table 3. Comparisons of the mean concentration (ng m^{-3}) of anhydrosugars, sugar, and sugar alcohols in Gosan aerosols with those from different sites around the world.

Sampling sites	Sampling type	Sampling time	Anhydro-sugars	Primary sugars	Sugar alcohols	References
Gosan, South Korea	TSP	Summer	3.74	22.8	14.3	This study
		Fall	25.9	38.3	13.4	
		Winter	48.0	20.2	2.60	
		Spring	15.7	90.0	7.36	
Chennai, India	PM ₁₀	Summer	127	15.5	7.44	Fu et al., 2010b
		Winter	134	11.4	4.81	
Mt. Tai, China	TSP	Summer (June)	224	61.1	125	Fu et al., 2012b
Alert, Canada	TSP	Winter	0.32	1.14	0.25	Fu et al., 2009a
		Spring	0.02	0.18	0.36	
Okinawa, western North Pacific	TSP	Summer	0.93	73.5	62.9	Zhu et al., 2015a, b
		Autumn	2.58	56.0	30.7	
		Winter	6.04	34.4	6.03	
		Spring	3.44	101	31.2	
Chichijima, western North Pacific	TSP	Summer	0.32	32.8	38.6	Verma et al., 2015, 2018
		Autumn	0.85	22.0	35.1	
		Winter	2.40	14.2	3.93	
		Spring	0.94	24.2	15.5	
Mt. Hua, China (Non-dust storm)	PM ₁₀	April	57.8	92.5	22.4	Wang et al., 2012
Mt. Hua, China (Dust storm)	PM ₁₀	April	44.5	162	25.7	Wang et al., 2012
Nanjing, China	PM _{2.5}	Summer	151 (Lev)	59.3	11.8	Wang and Kawamura, 2005
		Winter	268 (Lev)	42.3	13.4	
Beijing, China	PM _{2.5}	Summer	14.5	6.63	3.31	Kang et al., 2018a
		Autumn	129	17.2	13.7	
		Winter	254	41.5	17.8	
		Spring	81.4	33.9	12.3	
Belgrade, Serbia	TSP	Autumn	425 (Lev)	116	98.4	Zangrando et al., 2016
Maine, USA	PM ₁	May-October	13.9	28	8.31	Medeiros et al., 2006
Crete, Greece	PM ₁₀	Year-round	14.4	32.3	6.53	Theodosi et al., 2018

1127

1128

1129